Forest Ecology and Management 340 (2015) 135–152

Contents lists available at ScienceDirect

Forest Ecology and Management

journal homepage: www.elsevier.com/locate/foreco

Estimating weathering rates using base cation budgets in a Norway spruce stand on podzolised soil: Analysis of fluxes and uncertainties

Magnus Simonsson [a,*], Johan Bergholm [b,1], Bengt A. Olsson [c], Claudia von Brömssen [d], Ingrid Öborn [e,f]

[a] Department of Soil and Environment, Swedish University of Agricultural Sciences (SLU), P.O. Box 7014, SE-750 07 Uppsala, Sweden
[b] Kantarellvägen 6, SE-756 45 Uppsala, Sweden
[c] Department of Ecology, Swedish University of Agricultural Sciences (SLU), P.O. Box 7044, SE-750 07 Uppsala, Sweden
[d] Department of Economics, Unit of Applied Statistics and Mathematics, Swedish University of Agricultural Sciences (SLU), P.O. Box 7013, SE-750 07 Uppsala, Sweden
[e] Department of Crop Production Ecology, SLU, P.O. Box 7043, SE-750 07 Uppsala, Sweden
[f] World Agroforestry Centre, P.O. Box 30677-00100, Nairobi, Kenya

ARTICLE INFO

Article history:
Received 29 September 2014
Received in revised form 19 December 2014
Accepted 22 December 2014

Keywords:
Base cation
Cation budget
Weathering rate
Forest ecosystem
Combined standard uncertainty
The Skogaby experiment

ABSTRACT

Since forestry is often allocated to soils with a low weathering capacity, reliable estimates of weathering rates are crucial in analyses of sustainability, e.g. of whole-tree and stump harvesting. In the present study, weathering rates (kg ha^{-1} yr^{-1}) for base cations were estimated using cation budgets in a replicated ($n = 4$) experimental Norway spruce (*Picea abies* (L.) Karst.) plantation situated on a nutrient-poor glacial till in south-west Sweden and aged 25–39 years during the study period. Weathering rates (central values) were 2.4, 1.4, 0.3 and 2.3 kg ha^{-1} yr^{-1} for Ca, Mg, K and Na, respectively. However, weathering was a minor flux in the overall cycling of these cations in the ecosystem, and the confidence intervals of the weathering estimates had amplitudes that generally were greater than the central values. The overall uncertainties were divided into (i) regular standard errors of the mean, expressing spatial variability, sampling errors and random method-related errors in data from measurements replicated over the experimental plots ('Type A' uncertainties), and (ii) estimated standard uncertainties accounting for systematic errors of methods, and of uncertainties in variables, functions and factors not replicated over the plots ('Type B' uncertainties). For Ca and K, bioaccumulation dominated the overall uncertainty. Most (>90 %) of this uncertainty, in turn, was of Type A (between-plot variability in measured stem diameters and cation concentrations); the remainder resulted from Type B uncertainties in allometric functions etc. Hence, regular standard errors over plots yielded a correct level of uncertainty of weathering estimates for these ions at the studied site. For Mg and Na, however, deposition and leaching were large terms in the cation budget. Whereas the uncertainty in deposition was mostly taken into account by plot-wise replicated measurements of throughfall (Type A uncertainty), Type B uncertainties were crucial to the estimates of leaching. Due to the fact that uncertainties accumulate when terms are added and subtracted in a cation budget, it is difficult to predict the sustainability of the pools of exchangeable cations from estimated weathering rates; it may be better to measure them directly in the soil. However, in the studied ecosystem these had a rapid turnover (mean residence time, 1–4 years), and underwent abrupt fluctuations over only a few years. A study performed during a limited time may therefore suffer from considerable temporal uncertainties, if the results are to be generalised for a longer period.

1. Introduction

Weathering is a key process in the cycling of base cations, phosphorus and other elements in terrestrial ecosystems. Reliable estimates of weathering rates are crucial in analyses of the long-term sustainability of forest practices, and when assessing trends in soil and water quality under various scenarios of harvesting and deposition of air pollutants (e.g., Akselsson et al., 2007). For instance, estimates of weathering rates have been of fundamental importance in the calculation of critical loads of acidity to soils (e.g., Hodson and Langan, 1999). Forestry is often allocated to soils with low weathering rates, where negative base cation balances may impede long-term productivity. In particular, the introduction of more intensive harvesting practices in forestry, such as whole-tree

* Corresponding author. Tel: +46 18 67 12 72.
E-mail addresses: magnus.simonsson@slu.se (M. Simonsson), jabergholm@gmail.com (J. Bergholm), bengt.olsson@slu.se (B.A. Olsson), claudia.von.bromssen@slu.se (C.von Brömssen), i.oborn@cgiar.org (I. Öborn).
[1] Former address: Department of Ecology, Swedish University of Agricultural Sciences (SLU), P.O. Box 7044, SE-750 07 Uppsala, Sweden.

http://dx.doi.org/10.1016/j.foreco.2014.12.024
0378-1127/

and stump harvesting, may reduce the availability of plant nutrients at sites with a moderate or low inherent soil fertility (Thiffault et al., 2011). For instance, the study of Olsson et al. (1996) found it likely that whole-tree harvesting depletes base cations substantially in the forest floor of certain sites. This emphasises the importance of mineral weathering and stresses the requirement for an improved accuracy of weathering estimates (Klaminder et al., 2011). There is therefore a need to include base cation weathering in the planning of sustainable forest management. Biogeochemical simulation models, e.g. the PROFILE steady state model (Sverdrup and Warfvinge, 1993; Holmqvist et al., 2003), may be useful for estimating weathering rates over large areas. However, the quality of output data may be hampered by the often limited information regarding soil mineralogy, specific surface area and soil humidity. Furthermore, available versions have neglected the effects on surface reactivity of precipitates of secondary minerals and organic matter, and have failed to take account of micro-scale effects on weathering by exudates of roots and mycorrhiza ('biological weathering'). Hence, there is a need to improve existing modelling tools by validation against model-independent weathering estimates based on data from more or less intensively studied forest ecosystems.

Relevant methods include 'historical weathering' and ecosystem cation budgets (mass balances). In the former method, an element residing in highly weathering-resistant minerals, such as zirconium, is used as an internal standard for calculating mass losses of the more mobile elements in the soil profile (Olsson and Melkerud, 1989, 2000; Bain et al., 1993; Stendahl et al., 2013). In the cation budget method, weathering rates of base cations over a certain period are quantified from leaching, accumulation or losses in biomass and soil pools, inputs from atmospheric deposition and any application of fertiliser (as explained in Section 2.2.1). Hodson and Langan (1999) examined weathering rates for a Scottish moorland catchment, estimated by various methods, and concluded that reported and guesstimated uncertainties of the tested methods severely hampered the assessment of a critical load. Similar conclusions were reached by Klaminder et al. (2011) in a review of estimated calcium (Ca) and potassium (K) weathering rates for a forested catchment in northern Sweden: inconsistencies between estimates derived from different methods made them unreliable for predicting the effects of different harvesting intensities on soil nutrient pools.

It can be argued that all methods have their particular uncertainties, and possibly also biases, and cannot be expected to converge on a common weathering rate for a particular soil. Whereas historical weathering rates are interesting from a pedological viewpoint, because they yield an estimate of cumulative weathering since the onset of soil formation, cation budgets yield an estimate of the current weathering rate that may be more relevant for characterising the present flows in an ecosystem. Stendahl et al. (2013) pointed out that that millennial historical weathering rates should deviate substantially from current ones if weathering itself has altered the mineralogy of the soil. It therefore seems justified to analyse the precision within the methods, rather than across several ones. With these uncertainties known, it may be possible to draw conclusions from comparative studies on weathering rates in contrasting soils and/or land-use systems using a single method.

Cation budgets have been calculated at the scale of catchments (e.g., Koseva et al., 2010) as well as experimental plots (e.g., Andrist-Rangel et al., 2007; Simonsson et al., 2007; Öborn et al., 2010). In a soil cation budget, weathering is estimated by the difference from other independently measured element fluxes. Measurements of all these fluxes in forest ecosystems require substantial resources, time and patience. Sufficient data for estimating weathering rates are therefore available only for a limited number of study sites, where the original objectives were not necessarily to assess weathering. As weathering rates are estimated from the sum of several fluxes that are measured independently, the uncertainties of these will add up into the uncertainties of the weathering estimate (see Simonsson et al., 2007). For each process in the cation budget, there is a natural spatial and temporal variation in the environment, as well as errors that originate from sampling, sample preparation and chemical analyses etc. The influence of several of the many sources of uncertainty in an element budget have been addressed previously (Laclau et al., 2005; Yanai et al., 2010). However, there is currently a lack of any critical evaluation of the influence of the different terms and factors in cation budgets.

The aims of this study were: (i) to estimate weathering rates of calcium (Ca), magnesium (Mg), potassium (K), and sodium (Na) in an experimental forest using the cation budget method, and (ii) to analyse the sources of uncertainty in these estimates. The method took account of fluxes of deposition and leaching and accumulation in the growing biomass. In forest floor and mineral soil, changes in exchangeable cations were considered, but not of non-exchangeable cations. Special attention was paid to the partitioning of uncertainties on spatial variability and method errors expressed in standard errors over the experimental plots ('Type A' uncertainties), and the uncertainty of factors and functions that were generalised for all plots ('Type B' uncertainties), e.g. allometric biomass functions and systematic error when calculating the content of stones and boulders in the soil.

2. Materials and methods

2.1. Site characteristics

The study was conducted in the Skogaby forest experiment, which was an intensely studied field experiment designed to test the effect of deposition and nutritional conditions on the vitality and growth of trees. In 1913, the former *Calluna* moorland was planted with Scots pine (*Pinus sylvestris* (L.)). This stand was replaced by Norway spruce (*Picea abies* (L.) Karst.) in 1966. The site is located in southwest Sweden (56°33′20″N, 13°13′05″E) at 95–125 m above sea level and 17 km from the coast. The annual mean precipitation is 1100 mm and the annual mean temperature 7.6 °C. The area is exposed to deposition of anthropogenic sulphur (S) and nitrogen (N), as well as elements from a sea origin (Na, Mg, Cl, S, etc.), although the input of anthropogenic S and atmospheric acidity declined dramatically during the 1990s (Bergholm et al., 2003). The yearly mean open-field deposition of S and N for the period 1989–2001 was 11 and 17 kg ha^{-1} respectively.

The soil is a Haplic Podzol (FAO, 1990) developed on a loamy sandy till with approximately 4% clay (Table 1). The clay mineralogy, as described by Courchesne and Gobran (1997), is mainly vermiculitic and therefore poor in K-bearing phyllosilicates. The quantitative bulk mineralogy of the fine earth (<2 mm) shown in Table 1 was assessed in four plots (two of the control plots and two plots receiving ammonium sulphate applications) by spray drying of random powders according to Hillier (1999, 2003) and full-pattern fitting of X-ray diffraction patterns, similarly to participant 18 in Omotoso et al. (2006). Soil pH (H_2O) prior to the experimental treatments was 3.9 in the Oa-horizon, 4.1 in the upper 10 cm of the mineral soil, and 4.5 at 50 cm depth. The effective base saturation was 30 % in the Oa-horizon and varied from 8% to 12% in the top 50 cm of the mineral soil. Further physical and chemical characteristics of the soil were described by Bergholm et al. (1995). Organic matter constitutes virtually the entire humus layer and declines from 36 g kg^{-1} in the upper mineral soil, to 10 g kg^{-1} at 50 cm depth.

Table 1
Soil chemistry (pH, effective cation exchange capacity and base saturation: data from 1987 before the start of the experiment according to Bergholm et al., 1995); organic carbon (C) and nitrogen (N; average over all plots and years) texture (average over four locations in the experiment) and not previously published mineralogical composition of the fine earth (average over four investigated plots: two of the controls in this paper, and two ammonium-sulphate treated plots).

Depth (cm)	pH (H_2O)	CEC_{eff}	BS	Org C	Org N	Sand	Silt	Clay	Loss on ignition	Quartz	Plagioclase	K-feldspar	Amphibole	Muscovite	Biotite and phlogopite	Hydrobiotite	Vermiculite	Kaolinite	Smectite	Amorphous Fe oxides
		$cmol_c\ kg^{-1}$	%	$g\ kg^{-1}$	$g\ kg^{-1}$	Weight-% of fine earth				Weight-% of identified minerals in fine earth (<2 mm)										
FH-layer	3.91	24.0	29.8	417	15	–	–	–	–	–	–	–	–	–	–	–	–	–	–	–
0–5	4.07	5.6	8.4	36	1.5	61	29	5.2	5.2	52	22	19	1.9	0.2	0.00	0.74	1.09	0.33	1.73	1.07
5–10	"	"	"	"		61	29	5.2	5.2	53	22	19	2.1	0.5	0.01	0.26	0.89	0.01	0.62	1.35
10–20	4.44	3.5	6.9	24	1.1	61	28	5.1	5.4	53	22	18	2.5	0.6	0.09	0.35	1.00	0.26	0.37	1.84
20–30	4.46	2.7	8.3	20	1.0	61	30	4.5	4.6	50	23	19	3.0	0.9	0.04	0.76	1.06	0.09	0.45	2.09
30–40	4.51	1.9	11.0	14	0.70	62	31	3.5	3.7	46	24	19	3.8	1.1	0.39	0.94	1.24	0.32	0.71	2.45
40–50	4.54	1.4	12.4	10	0.50	65	29	3.1	2.9	49	25	19	3.7	1.1	0.15	0.25	1.20	0.00	0.00	1.73
50–60	–	–	–	–	–	64	30	2.8	2.5	49	25	19	3.5	0.9	0.29	0.08	0.65	0.00	0.00	1.28
60–70	–	–	–	–	–	70	26	2.3	1.4	50	25	19	3.2	0.8	0.21	0.00	0.42	0.00	0.00	1.09
70–80	–	–	–	–	–	65	30	2.8	1.7	51	25	19	3.2	0.7	0.19	0.00	0.45	0.00	0.00	0.94
80–90	–	–	–	–	–	64	31	2.8	1.6	51	25	19	3.2	0.8	0.16	0.00	0.46	0.00	0.00	1.05
90–100	–	–	–	–	–	71	25	3.0	0.9	51	25	19	3.1	0.6	0.16	0.00	0.37	0.00	0.00	0.98

In 1988, a randomised block ($n = 4$) experiment was started with treatments including nitrogen-free fertilisation, irrigation, irrigation fertilisation and drought (Nilsson and Wiklund, 1994; Bergholm et al., 1995). At the start of the experiment, the age of the Norway spruce trees was 25 years, including three years in the nursery. Treatments and control (no treatment) were applied in plots of 45 m by 45 m (2025 m^2) with a smaller 'net plot' inside each plot, which was used for measuring tree growth, throughfall and litterfall. At the start of the experiment, the net plot was 12.5 m by 12.5 m (156 m^2). In 1993, the stand was thinned by removing 25% of the basal area, which corresponded to a reduction of the biomass by 14% on average. At the same time, the net plot was increased to 30 m by 30 m (900 m^2).

2.2. Weathering rate estimated from the cation budget

2.2.1. The cation budget

This work was constrained to a study period of 14 years, 1987–2001, for which data were available that permitted to calculate a cation budget. The data presented here were restricted to the four control plots. A mean annual weathering rate was calculated using Eq. (1a):

$$\mathrm{Weath}_i = -\mathrm{Dep}_i + \Delta\mathrm{Exch}_i + \mathrm{Leach}_i + \mathrm{Bioacc}_i \quad (1a)$$

The components denoted by subscript '*i*' were individual base cations (Ca, Mg, K, and Na; $kg\ ha^{-1}\ yr^{-1}$) and their equivalent sum (ΣBC; $kmol_c\ ha^{-1}\ yr^{-1}$). The terms are, in the order of appearance in Eq. (1a), rates of weathering, deposition, change in exchangeable cations in forest floor and mineral soil (the latter at 0–50 cm depth), leaching and accumulation in the biomass. Changes in non-exchangeable pools of, e.g., Ca in the forest floor, or fixed K in clay minerals, were not considered. Hence, 'weathering' in this study may comprehend any mobilisation from or accumulation in soil pools other than the exchange complex in the investigated part of the soil profile.

It was noticed that the terms of Eq. (1a) were not independent. This was particularly obvious for deposition and leaching. Therefore, Weath_i in Eq. (1a) was calculated separately for each plot, before calculating a mean of each Weath_i over the four plots.

2.2.2. Overall uncertainty of the cation budget

Temporal variability in the data was not considered as a measure of uncertainty in the current investigation. The regular standard error (SE) of the mean Weath_i over the four plots would accounted for spatial variability, sampling errors and random methodological errors in measurements replicated over the four plots, henceforth referred to as 'Type A' uncertainties. However, all terms in Eq. (1a) were at least partly based on general factors, models or estimates that were not determined independently in the four plots. The uncertainties in these had to be estimated separately, as described in Section 2.3–2.6, and are referred to below as 'Type B' uncertainties. Our approach was to calculate Eq. (1a) plot-wise in a Monte Carlo manner, and then to calculate the mean and SE of Weath_i over the four plots. Each term in Eq. (1a) had a central value for the plot of interest and a Type B error. The mean weathering for a cation (subscript '*i*') over the four plots ('*p*') was formulated as:

$$\mathrm{Weath}_i = \frac{1}{4}\sum_{p=1}^{4}\{[-\mathrm{Dep}_{i,\ p} \pm \varepsilon_{\mathrm{Type\ B}}(\mathrm{Dep}_i)] + [\Delta\mathrm{Exch}_{i,\ p} \pm \varepsilon_{\mathrm{Type\ B}}(\Delta\mathrm{Exch}_i)] + [\mathrm{Leach}_{i,\ p} \pm \varepsilon_{\mathrm{Type\ B}}(\mathrm{Leach}_i)] + [\mathrm{Bioacc}_{i,\ p} \pm \varepsilon_{\mathrm{Type\ B}}(\mathrm{Leach}_i)]\} \quad (1b)$$

Eq. (1b) was computed 1000 times in a Monte Carlo fashion, where the error terms, '$\varepsilon_{\text{Type B}}$', were the relevant errors due to Type B uncertainties. The '$\varepsilon_{\text{Type B}}$' terms were derived from an analysis of the overall uncertainty in the mean over the four plots for each term in the cation budget. These overall uncertainties, or 'combined standard uncertainties', u_c (ISO, 1995), corresponded to a standard error of the mean including both Type A and B uncertainties. The 'u' notation for 'uncertainty' will consistently be used for Type B standard uncertainties, partly or entirely derived from other sources than ordinary replication over the plots. The portion of each u_c that resulted from Type B uncertainties, $u_{\text{Type B}}$, was assessed and multiplied by $\sqrt{4}$, to make it relevant for every single plot in Eq. (1b). In each round of the Monte Carlo, every $\varepsilon_{\text{Type B}}$ was the corresponding product $\sqrt{4} \times u_{\text{Type B}}$ multiplied by a normally distributed random number with a mean of zero and standard deviation of one.

Each of the 1000 realisations yielded a mean Weath_i over the four plots and a standard error of the mean. The median mean and the median standard error were taken as Weath_i and an 'extended standard error' of weathering, $\text{SE}_{\text{extended}}(\text{Weath}_i)$, respectively. The latter contained both Type A and B uncertainties. By switching all '$\varepsilon_{\text{Type B}}$' terms off, we also estimated the traditional Type A standard error, $\text{SE}(\text{Weath}_i)$. Turning back to the extended standard error, the contribution of each cation budget term was estimated by replacing all bracketed terms of Eq. (1b), except the one under consideration, with the relevant means over the four plots. The resulting partial standard error was squared and divided by $(\text{SE}_{\text{extended}}(\text{Weath}_i))^2$, to yield the contribution of the non-fixed variable as a percentage at the squared (variance) scale. As the sum of individual contributions deviated from 100%, and the terms in the cation budget can be expected to be correlated, we considered the remaining positive or negative part as a 'covariance' contribution.

Table 2 gives a summary of standard errors and standard uncertainties identified in the study, and may provide satisfactory background for reading the Results. The following Sections 2.3–2.6 describe in detail how the budget terms and their uncertainties were derived for each of the terms in the cation budget.

2.3. Deposition of base cations

2.3.1. Deposition rates

The wet and dry deposition of base cations was measured from January 1989 to June 1999. Open-field deposition was sampled in four collectors in a nearby open-field. Throughfall was collected in six collectors located within each plot. The collectors consisted of a polythene funnel, 20 cm in diameter, connected to a container placed in a dark box. Open-field collectors were placed 3 m above the ground, and throughfall collectors were placed on the forest floor. Deposition was collected every fortnight during June–September, and every month during the rest of the year. The samples were stored in a freezer (−18 °C) prior to chemical analysis with atomic absorption and atomic emission spectrometry (AAS, AES; 1989–1993) or inductively coupled plasma emission spectroscopy (ICP-ES; 1994–1999). The analysis took place with no prior acid digestion, and hence included only dissolved cations and dry deposition of readily soluble salts. Agreement (no significant differences) between analyses (AAS and AES vs. ICP-ES) was reported by Bergholm et al. (2003).

On each sampling occasion, samples were pooled by volume to yield one sample of open-field solution in total, and one throughfall solution per plot. Sample volumes were multiplied by the concentrations in the samples to yield fluxes of the cations. Annual deposition was obtained by totalling all the sampling occasions of the year of interest.

Table 2
Terms in the cation budget and their sources of uncertainties divided into 'Type A' uncertainties derived from standard errors over the four plots (shown as absolute or relative standard errors of the mean, 'SE' and 'SE_{rel}') and 'Type B' uncertainties ('u' or 'u_{rel}') that had to be added to yield the extended standard error of weathering rates.

Term in balance	Type A uncertainties: Standard errors of the mean over plots ($n = 4$)	Type B uncertainties: Additional standard uncertainties, for average plot estimates
Deposition	$\text{SE}(\text{Dep}_i)$ derived from plot-wise measured throughfall of Na; $\text{SE}_{\text{rel}}(\text{TF}_{\text{Na}}) = 12.5$ %	Estimated uncertainty of open-field deposition of individual cations or their equivalent sum ('i'), $u_{\text{rel}}(\text{OF}_i) = 1.6$–$2.2$%; in addition, positive covariance of OF_i with open-field deposition of Na and with throughfall of Na
Change in exchangeable cations	Standard error for individual cations or their equivalent sum ('i'), $\text{SE}(\Delta\text{Exch}_i)$, accounting for between-plot variability in: • Cation concentrations in mineral soil horizons and humus (FH) layers all years; in litter (L) layers 1993, 1997 and 2001 • Mass of humus FH-layers all years; of L-layers 1993, 1997 and 2001 • Content of gravel in individual plots and horizons; of stones and boulders in individual plots	Additional uncertainties, $u_{\text{Type B}}(\Delta\text{Exch}_i)$, accounting for: • Errors in extrapolated L/FH-ratios, used to estimate missing data for exchangeable cations in the litter L-layer in early years (1987, 1990) • Errors in using horizon-wise average, rather than plot-wise, dry bulk densities of mineral soil materials <20 mm, $\rho_{<20\ \text{mm},\ z}$ (standard deviations 8–26% of the nominal value) • Systematic error in the soil's content of stones and boulders, SB_p: Published uncertainty of 9 percentage units (by volume) applied for the whole site.
Leaching	$\text{SE}(\text{Leach}_i)$ derived from plot-wise measured concentrations of individual cations or their equivalent sum in soil water at 50 cm depth, $\text{SE}_{\text{rel}}(\text{Conc}_i) = 3$–$19$%	Guesstimated uncertainty of modelled water flux, $u_{\text{rel}}(\text{Flux}) = 10$%
Bioaccumulation: biomass	Stem diameter measurements, $\text{SE}_{\text{rel}}(W_j) = 6$–$11$% for individual tree compartments ('j') in individual years	Relative standard uncertainty when applying allometric functions for estimating the average biomass of compartment ('j') over the four plots, $u_{\text{rel, allometric}}(W_j)$, obtained by Monte Carlo calculations based on RMSE of regressions developed within the Skogaby experiment (stem, needles, living branches, dead branches) or from literature (stumps and roots); see Table 3 Relative standard uncertainty in ratio of bark to total stem biomass, evaluated from data within the Skogaby experiment, $u_{\text{rel}}(\text{Bark/Stem}) = 4.4$%
Bioaccumulation: cation concentrations	Relative standard errors in concentrations of individual cations or their equivalent sum ('i') in individual tree compartments ('j'): $\text{SE}_{\text{rel}}(\text{Conc}_{ij}) = 0.4$–$23$% based on standard errors over the four plots analysed in 1993 and 2001 (needles, living branches, dead branches)	Systematic error in the assumption that cation concentration in stumps and roots equalled the mass-weighted average of concentrations in above-ground stem wood and stem bark: guesstimated $u_{\text{rel}}(\text{Stump-root conc}) = 10$%

The deposition input of Na to the ecosystem was directly obtained from the throughfall of this element, which includes wet deposition and dry deposition captured by the tree canopy. The other base cations, Ca, Mg and K, undergo considerable biocycling through uptake by roots followed by excretion from the canopy; hence throughfall does not represent the input to the ecosystem. Instead, open-field bulk (total) deposition was used after correction for additional (dry) deposition captured by the tree canopy using the 'Na ratio method' (e.g., Lövblad et al., 2000). The method postulates: that the canopy has the same influence on the total input of all base cations, and that the tree canopy does not excrete any Na. The total deposition ('Dep') input (kg ha^{-1} yr^{-1}) of a cation ('*i*') in a plot ('*p*') was given from the open field deposition of the same cation (OF_i), and the ratio of Na throughfall in the plot and open field deposition of Na ($TF_{Na,\ p}/OF_{Na}$), using Eq. (2):

$$Dep_{i,\ p} = OF_i \times \frac{TF_{Na,\ p}}{OF_{Na}} \quad (2)$$

An analogous calculation was performed for chloride, which was analysed in throughfall and open-field waters with ion chromatography, for comparison with the leaching of this presumably biogeochemically inert element. The total base cation deposition input to a plot, $Dep_{\Sigma BC}$ (kmol$_c$ ha^{-1} yr^{-1}), was obtained by inserting the equivalent sum of base cations instead of OF_i in Eq. (2).

$TF_{Na,\ p}$ was calculated as an average annual flux over the years 1989–2001 within each of the four plots. OF_{Na} was the average annual flux obtained in the bulked open-field samples; the same applies for Ca, Mg and K. The annual average throughfall of Na ranged from 24 to 40 kg ha^{-1} yr^{-1} among the plots, whereas the open field deposition of Na had an average of 18 kg ha^{-1} yr^{-1}, meaning that the ratio of $TF_{Na,\ p}/OF_{Na}$ in Eq. (2) was in the range 1.3–2.2.

From June 1999 to the end of 2001, deposition was estimated from the annual precipitation at a nearby meteorological station (Åbacken) combined with annual mean concentrations in open-field and throughfall solutions from a nearby spruce site (Timrilt), which had a stand similar to that at Skogaby. Concentrations had previously been calibrated against values for Skogaby during 1994–1998 using a linear regression equation with a high explanatory power (R^2 = 0.977).

2.3.2. Combined standard uncertainty of the deposition rates

Besides plot-wise $Dep_{i,\ p}$, the average plot Dep_i was calculated and its combined standard uncertainty estimated. For the deposition of Na, the standard error in Na throughfall over the four plots, $SE(TF_{Na})$, was used without further processing. Obtained by replication over the four plots, it was considered a Type A uncertainty. For the other base cations, uncertainties were combined from the components in Eq. (2). A relative combined standard uncertainty of the element of interest, $u_{c,\ rel}(Dep_i)$, was calculated from the relative standard error (standard error divided by the mean) of Na throughfall, $SE_{rel}(TF_{Na})$, and estimated relative standard uncertainties for the remaining fluxes in Eq. (2), $u_{rel}(OF_i)$ and $u_{rel}(OF_{Na})$. Additional contributions from covariance of the three fluxes were taken into account following Castrup (2004) and the guide 'Quantifying Uncertainty in Analytical Measurement', available from the Eurachem website http://www.eurachem.org/; Eq. (3):

$$u_{c,\ rel}(Dep_i) = \left[\begin{array}{l} (SE_{rel}(TF_{Na}))^2 + (u_{rel}(OF_i))^2 + (u_{rel}(OF_{Na}))^2 \\ +2r(TF_{Na}, OF_i) \times SE_{rel}(TF_{Na}) \times u_{rel}(OF_i) \\ +2r(TF_{Na}, OF_{Na}) \times SE_{rel}(TF_{Na}) \times u_{rel}(OF_{Na}) \\ +2r(OF_i, OF_{Na}) \times u_{rel}(OF_i) \times u_{rel}(OF_{Na}) \end{array} \right]^{1/2} \quad (3)$$

The correlation coefficients, '*r*' for each pair of variables, were estimated from variations over time during the study period. Addition of squared relative (rather than absolute) standard uncertainties is the procedure to use for a variable that is obtained by multiplication and/or division as in Eq. (2) (see ISO, 1995, and the Eurachem guide mentioned above). The correlation coefficients ranged from 0.5 to 0.9, and $u_{c,\ rel}(Dep_i)$ was close to the arithmetic sum of $SE_{rel}(TF_{Na}) + u_{rel}(OF_i) + u_{rel}(OF_{Na})$.

For the open-field deposition values, a standard uncertainty was estimated based on electrical conductivity, which had been recorded in the individual open-field collectors in 1998. By using the Marion–Babcock equation (Sposito, 1989), the electrical conductivity was transformed into an ionic strength for each sampling occasion. By multiplying the estimated ionic strength by the water volume of each sampling occasion, a volume–weighted ionic strength for the year 1998 was obtained for each collector. Over the four collectors, the relative standard deviation was only 2.4%. For throughfall, the cumulative ionic strength had a much larger relative standard deviation: 14% over the four plots in the same year. Assuming that individual ions and their equivalent sum generally varied in analogy with accumulated ionic strengths this particular year, relative standard uncertainties for open field deposition of the individual cations and for their equivalent sum, $u_{rel}(OF_i)$, were estimated by multiplying the relevant throughfall standard error, $SE_{rel}(TF_i)$, by the ratio 2.4/14.

For each cation, the relative combined standard uncertainty, $u_{c,\ rel}(Dep_i)$, obtained from Eq. (3), was converted to an absolute $u_c(Dep_i)$ by multiplication by the mean over the four plots, Dep_i:

$$u_c(Dep_i) = u_{c,\ rel}(Dep_i) \times Dep_i \quad (4)$$

The plot-wise replicated throughfall of Na constituted the Type A standard error of Dep_i, calculated as:

$$SE(Dep_i) = SE_{rel}(TF_{Na}) \times Dep_i \quad (5)$$

Its relative contribution (percentage) to the combined standard uncertainty was calculated at the squared (variance) scale using Eq. (6):

$$Contribution_{Dep_i}\ (TF_{Na}) = \frac{(SE_{rel}(TF_{Na}))^2}{(u_{c,\ rel}(Dep_i))^2} \quad (6)$$

Absolute and relative contributions from the open-field items in Eq. (3) were calculated analogously, by inserting $u_{rel}(OF_i)$, etc. instead of $SE_{rel}(TF_{Na})$ in Eqs. (5) and (6).

As to the deposition based on nearby sites during June 1999 to December 2001, it was assumed that any additional uncertainty due to this procedure was negligible.

2.4. Exchangeable base cations

2.4.1. Rate of change in exchangeable base cations

Soil samples were taken in October on five occasions: in 1987 (prior to the start of the experiment) and then in 1990, 1993, 1997 and 2001. Volume-based composite samples of forest floor were obtained by combining 40 subsamples per plot taken with a steel cylinder (5.6 cm diameter). From 1993, forest floor samples were split into litter (L) and humus (FH) layers, which were weighed and analysed separately; in 1987 and 1990, only the FH-layer was sampled. Mineral soil composite samples, based on 20 sub-samples per plot, were taken to a 50-cm depth using a soil core sampler (2.8 cm diameter), and divided into five 10-cm layers. The samples were stored fresh at +8 °C prior to further processing.

The composite samples, one per plot and per layer, were sieved fresh; L- and FH-materials through a 6 mm mesh, and mineral soil through a 2 mm mesh. Exchangeable base cations were analysed using AAS in early years and ICP-ES in later years after extraction

of fresh soil samples with 1 M NH_4Cl; see details in Bergholm et al. (2003).

The cation concentrations of each soil level were multiplied by the surface-related mass (kg ha^{-1}) of forest floor materials (L- and FH-layers) or fine earth (<2 mm, mineral soil), as relevant for the sample of interest, to yield surface-related masses of exchangeable cations (kg ha^{-1}). These masses were then added to 50 cm depth for each plot and year; Eq. (7a).

$$\mathrm{Exch}_{i,\,p} = \mathrm{Exch}_{i,\,p,\,\mathrm{L}} + \mathrm{Exch}_{i,\,p,\,\mathrm{FH}} + \sum_{z=0-10\ \mathrm{cm}}^{40-50\ \mathrm{cm}} \left(c_{i,\,p,\,z}\, m_{p,\,z}\right) \tag{7a}$$

$\mathrm{Exch}_{i,\,p}$ is the content of cation '*i*' in the profile of plot '*p*'; $\mathrm{Exch}_{i,\,p,\,\mathrm{L}}$ and $\mathrm{Exch}_{i,\,p,\,\mathrm{FH}}$ are the cation content in the L- and FH-layers, respectively; $c_{i,\,p,\,z}$ is the cation concentration in the fine earth (<2 mm) of layer '*z*' in the mineral soil of plot '*p*'; $m_{p,\,z}$ is the surface-related mass of fine earth (<2 mm) in the same layer. Implicit in Eq. (7a) are surface-related masses of L- and FH-layers, which were determined from the combined dry-weights of the 40 cores from each plot and sampling occasion. For the mineral soil, the surface-related fine earth (<2 mm) was determined using the dry bulk density of materials finer than 20 mm ('$\rho_{<20\ \mathrm{mm}}$'; kg m^{-3}), the volumetric content of stones and boulders ('SB'; $m^3\ m^{-3}$ of materials >20 mm), and the content of gravel in the <20 mm fraction ('$m_{2-20\ \mathrm{mm}}/m_{<20\ \mathrm{mm}}$'; kg kg^{-1}). With these quantities known, the mass of fine earth of layer '*z*' in plot '*p*' ($m_{p,\,z}$; kg ha^{-1}) can be calculated from Eq. (8); V_z is the volume of the layer of interest (1000 $m^3\ ha^{-1}$ for a 10-cm layer):

$$m_{p,\,z} = V_z \rho_{<20\ \mathrm{mm},\,z}\,(1 - \mathrm{SB}_p)\left(1 - \frac{m_{2-20\ \mathrm{mm},\,p,\,z}}{m_{<20\ \mathrm{mm},\,p,\,z}}\right) \tag{8}$$

Dry bulk densities were obtained on one single occasion from steel cylinders (height 50 mm, inner diameter 72 mm) inserted vertically at every 5 cm depth interval from 5–10 cm to 45–50 cm in the mineral soil, thereby avoiding to include stones (>20 mm) in the samples. This was done in four pits dug at locations that did not coincide with the control plots of the present study. Wherever possible, two cylinders were inserted at every depth in each pit. As indicted by the subscript indices of the dry bulk density in Eq. (8), a mean value was used for each depth, rather than plot-wise values. The content of stones and bolders, SB_p, was determined over the entire area of each control plot, yielding a general value for 0–50 cm depth. This was done using the rod method of Viro (1952), in which the penetration depth (average within the plot) of a standardised steel rod is converted into a content of stones and boulders in the upper 30 cm, which was assumed valid for the profile to 50 cm depth. The content of gravel in the <20 mm fraction was obtained by sieving and weighing soil from each 10-cm layer within a 0.25 m^2 area, from 0 to 50 cm depth into the mineral soil, in a pit dug in each control plot.

Eq. (7a) could be applied directly for the years 1993, 1997 and 2001. For 1987 and 1990, exchangeable cations in the lacking L-layers from 1987 and 1990 were estimated using cation contents of the FH-layer, $\mathrm{Exch}_{i,\,p,\,\mathrm{FH}}$, and estimates of the ratio $\mathrm{Exch}_{i,\,\mathrm{L}}/\mathrm{Exch}_{i,\,\mathrm{FH}}$ for each year, 'L/FH-ratio' in Eq. (7b).

$$\mathrm{Exch}_{i,\,p} = \mathrm{Exch}_{i,\,p,\,\mathrm{FH}}(\mathrm{L/FH\text{-}ratio}_i + 1) + \sum_{z=0-10\ \mathrm{cm}}^{40-50\ \mathrm{cm}} \left(c_{i,\,p,\,z}\, m_{p,\,z}\right) \tag{7b}$$

According to data from 1993 to 2001, these ratios, with an overall range of 0.01–0.33 (average 0.10), did not differ significantly between plots, but did so for the different cations, and declined with time for all elements ($P < 0.05$ for regressions on year for Ca, Mg, K, Na and ΣBC). Extrapolated ratios were calculated for 1987 and 1990 using linear regression, one for each cation and year but common for all plots.

For each plot, a regression on time of $\mathrm{Exch}_{i,\,p}$, summed up according to Eq. (7a) or (7b), was calculated to yield a mean annual change for individual cations (kg $ha^{-1}\ yr^{-1}$) and their equivalent sum (kmol$_c$ $ha^{-1}\ yr^{-1}$); $\Delta\mathrm{Exch}_{i,\,p}$, used in Eq. (1b).

2.4.2. Combined standard uncertainty of the rate of change in exchangeable base cations

Over the four plots, the average slope with respect to time, $\Delta\mathrm{Exch}_i$, with standard error of the mean, $\mathrm{SE}(\Delta\mathrm{Exch}_i)$, was calculated. The latter was the Type A uncertainty, which accounted for plot variability regarding cation concentrations and masses of soil solids in the FH-layer all years, and in the L-layer in later years, in the forest floor; in the mineral soil, it accounted for between-plot variability in cation concentrations and partly for the variability (uncertainty) in surface-related mass of mineral soil, owing to the use of plot-wise values for stones, boulders and gravel in Eq. (8). Type B uncertainty had to be added for the extrapolated cations in the L-layer in 1987 and 1990, for bulk densities that were generalised over the plots, and for the expected systematic error in the content of stones and boulders in the soil profile. Deriving analytical expressions that accounted for the various Type B uncertainties in Eqs. (7a) and (7b), and the underlying Eq. (8), was impractical. Instead, we used a spreadsheet solution designed to quantify the change in $\Delta\mathrm{Exch}_i$ when each variable having a Type B uncertainty was shifted one standard uncertainty away from its nominal value. The square root of the sum of squares in $\Delta\mathrm{Exch}_i$ (one squared change per shifted variable) was equivalent to the Type B standard uncertainty of the nominal mean change obtained from the four plots, $u_{\mathrm{Type\ B}}(\Delta\mathrm{Exch}_i)$. The combined standard uncertainty, $u_c(\Delta\mathrm{Exch}_i)$, was finally calculated as:

$$u_c(\Delta\mathrm{Exch}_i) = \left[(\mathrm{SE}(\Delta\mathrm{Exch}_i))^2 + (u_{\mathrm{Type\ B}}(\Delta\mathrm{Exch}_i))^2\right]^{1/2} \tag{9}$$

As to the components of this calculation, extrapolated L/FH-ratios for each element in Eq. (7b) occurred on two occasions (the years 1987 and 1990) and in four plots. Each of these eight occurrences was treated as an independent realisation of 'L/FH-ratio$_i$' in Eq. (7b), with a nominal value, as predicted for the year and cation of interest from the linear regression, and standard uncertainty, $u(\mathrm{L/FH\text{-}ratio}_i)$, obtained from conventional theory of linear regression (e.g., Mead et al., 1993):

$$u(\mathrm{L/FH\text{-}ratio}_i) = \left[\mathrm{RMSE}_i^2\left(1 + \frac{1}{n_{\mathrm{cal}}} + \frac{\left[\mathrm{Year} - \overline{\mathrm{Year}_{\mathrm{cal}}}\right]^2}{\mathrm{SS(Year)}_{\mathrm{cal}}}\right)\right]^{1/2} \tag{10}$$

In Eq. (10), RMSE_i is the root mean square error (residual) of the regression for the cation of interest in the calibration ('cal') data from 1993 to 2001, based on $n_{\mathrm{cal}} = 12$ observations (4 plots, 3 occasions); Year is 1987 or 1990, for which the ratio was estimated; $\overline{\mathrm{Year}_{\mathrm{cal}}}$ and $\mathrm{SS(Year)}_{\mathrm{cal}}$ are the mean and sum of squares of Year in the calibration data, respectively. Although $u(\mathrm{L/FH\text{-}ratio}_i)$ was based on data replicated in the plots, we considered it as a Type B uncertainty, because it was used to estimate missing data in Eq. (7b).

The 20 occurrences of bulk densities (4 plots, 5 depths) were treated as independent realisations, each with a nominal value equal to the mean bulk density from the depth of interest, $\rho_{<20\ \mathrm{mm},\,z}$, and a standard uncertainty (random error) equal to the standard deviation over all cylinders available from the depth of interest. Dry bulk densities were 1124 kg m^{-3} on average, with a typical standard deviation of 146 kg m^{-3}.

As to the volumetric content of stones and boulders, Stendahl et al. (2009) reported a root mean square error of prediction of 9.2–9.5 percentage units (by volume) for an individual site. According to Eriksson and Holmgren (1996), approximately 90% of this uncertainty is caused by limitations and errors in the method, rather than sample errors, due to the fact that the method is unable to cope with site-specific peculiarities regarding size and distribution of boulders in the profile. In the spreadsheet solution, the content of stones and boulders of all plots were assigned a systematic error of 9 percentage units for the whole site. It was done by multiplying each plot-specific SB_p by a common coefficient, which had the nominal value of one and a standard uncertainty of 0.09. The content of stones and boulders was in the range 24–36% by volume; the gravel ranged from 1% to 17% by weight of materials <20 cm.

2.5. Leaching of base cations

2.5.1. Rate of leaching

Leaching losses were assumed to equal the vertical flux of base cations at 50 cm depth. Each plot had six suction lysimeters equipped with ceramic cups of P80 material (CeramTec, Germany) and installed at 50 cm depth. The lysimeters were operated at a transient vacuum for one week using an initial tension of about −70 kPa. During 1989–1990, soil solutions were collected up to 11 times per year, and thereafter 3–4 times per year, in spring and autumn depending on soil water supply which varied between years and plots. Soil solution samples were pooled by weight, yielding one sample per plot and sampling occasion. The samples were stored in a freezer (−18 °C) prior to analysis using ICP-ES. A general daily flux of soil water, pertaining to all the studied plots, was estimated using the SOIL-model (Jansson, 1998). The model consists of two differential equations describing the vertical flux of water and heat, with daily mean air temperature, air humidity, wind speed and global radiation as driving variables.

Daily element leaching from 50 cm depth was calculated as the concentration of each element, linearly interpolated on a daily basis between sampling occasions, multiplied by the modelled daily flux of soil water at the same depth. For each plot, summation over days yielded an estimate of annual leaching for each year, and the mean across all years yielded the annual leaching during the experimental period. To avoid systematic error in the difference between leaching and deposition in Eq. (1b), cation leaching rates were corrected based on the leaching of chloride (Cl). We assumed that the leaching of Cl should be equal to the deposition, and multiplied the uncorrected mean annual cation leaching from each plot, $\mathrm{Leach}_{\mathrm{uncorr},\,i,\,p}$, by the ratio of deposition to leaching for chloride for the plot of interest, $\mathrm{Dep}_{\mathrm{Cl},\,p}/\mathrm{Leach}_{\mathrm{Cl},\,p}$; Eq. (11):

$$\mathrm{Leach}_{i,\,p} = \mathrm{Leach}_{\mathrm{uncorr},\,i,\,p} \times \frac{\mathrm{Dep}_{\mathrm{Cl},\,p}}{\mathrm{Leach}_{\mathrm{Cl},\,p}} \tag{11}$$

2.5.2. Combined standard uncertainty of the rate of leaching

In the lack of plot-wise data for water fluxes, an average leaching, Leach_i, and a standard error, $\mathrm{SE}(\mathrm{Leach}_i)$, were calculated over the four plots. The latter was a Type A uncertainty that only expressed the spatial variability in measured concentrations. It failed to take account of the uncertainty in modelled water runoff, which was therefore a Type B uncertainty. The relative version, $\mathrm{SE}_{\mathrm{rel}}(\mathrm{Leach}_i)$, was therefore considered as a relative standard error of the concentrations, $\mathrm{SE}_{\mathrm{rel}}(\mathrm{Conc}_i)$. As to uncertainties in the modelled water flux, preliminary Monte Carlo calculations showed only negligible effects of randomised errors in the daily fluxes. The errors tended to cancel themselves out over extended periods. To test the sensitivity for bias remaining after the correction of leaching using chloride, an overall guesstimated relative standard uncertainty of 10% was applied as a systematic error for the whole experimental period, $u_{\mathrm{rel}}(\mathrm{Flux})$. The uncertainties of concentrations and fluxes were added to a combined relative standard uncertainty for leaching of each cation, $u_{c,\,\mathrm{rel}}(\mathrm{Leach_i})$, according to Eq. (12):

$$u_{\mathrm{c,\,rel}}(\mathrm{Leach}_i) = \left[(\mathrm{SE}_{\mathrm{rel}}(\mathrm{Conc}_i))^2 + (u_{\mathrm{rel}}(\mathrm{Flux}))^2\right]^{1/2} \tag{12}$$

The data did not permit to establish any correlation between the two variables. Therefore, the uncertainties in Eq. (12) had to be added without correction for covariance. Absolute combined standard uncertainties, $u_{\mathrm{c}}(\mathrm{Leach}_i)$, were obtained by multiplying $u_{\mathrm{c,\,rel}}(\mathrm{Leach}_i)$ by the average over the plots, Leach_i, similarly to Eq. (4). The Type B portion, $u_{\mathrm{Type\ B}}(\mathrm{Leach}_i)$, was calculated in analogy with Eqs. (5) and (6).

2.6. Base cations accumulated in biomass

2.6.1. Rate of bioaccumulation

Bioaccumulation of Ca, Mg and K (kg ha^{-1} yr^{-1}) and their equivalent sum (kmol$_c$ ha^{-1} yr^{-1}) were estimated in six tree compartments (pools): stem wood, stem bark, needles, living branches, dead branches, and stumps and roots. The annual accumulation rate of each cation in the average plot was obtained by adding together the pools and dividing by the 14 years of the study period (1987–2001). More precisely, two periods had to be considered: one 'pre-thinning' period from 1987 to 1993, and one 'post-thinning' period from 1993 to 2001. Upon thinning, all parts of the felled trees were removed from the plots, except stumps and roots. Any base cation flux back to the soil from stumps and roots left in the plots upon thinning was ignored. Using Eq. (13), the overall annual bioaccumulation of a cation ('*i*') of a plot ('*p*') was calculated by summing over the relevant pools, each associated with a tree compartment ('*j*') and a sampling occasion (e.g., '$[\mathrm{Pool}_{i,\,j,\,p}]_{1999,\ \text{pre-thinning}}$' for cation '*i*' in tree compartment '*j*' in plot '*p*' before the thinning in 1993):

$$\mathrm{Bioacc}_{i,\,p} = \frac{1}{14} \times \sum_j \Big\{ [\mathrm{Pool}_{i,\,j,\,p}]_{1993,\ \text{pre-thinning}} - [\mathrm{Pool}_{i,\,j,\,p}]_{1987} + [\mathrm{Pool}_{i,\,j,\,p}]_{2001} - [\mathrm{Pool}_{i,\,j,\,p}]_{1993,\ \text{post-thinning}} \Big\} \tag{13}$$

Each $\mathrm{Pool}_{i,\,j,\,p}$ in Eq. (13) was calculated by multiplying year-specific values for dry weight biomass, $W_{j,\,p}$ (kg ha^{-1}), and element concentrations in the biomass, $\mathrm{Conc}_{i,\,j,\,p}$, according to Eq. (14a).

$$\mathrm{Pool}_{i,\,j,\,p} = W_{j,\,p} \times \mathrm{Conc}_{i,\,j,\,p} \tag{14a}$$

To estimate the biomass, stem diameters at chest height (1.3 m above ground) were measured yearly for all trees in the experiment using a calliper. The biomass of individual trees was calculated using allometric regressions, where the logarithmic biomass of compartments ('*j*') in individual trees ('*k*'), $\ln(W_{j,\,k})$, was obtained as a function of logarithmic stem diameter only, $\ln(D)$ (Table 3). Back-transformation to arithmetic biomass values was performed with log-linear bias correction according to Baskerville (1971); Eq. (15) for tree compartment ('*j*'):

$$W_{j,\,k} = \exp\{\ln(W_{j,\,k}) + 1/2 \times [\mathrm{RMSE}_j \times (\ln(W_{j,\,k}))]^2\}, \tag{15}$$

where $W_{j,\,k}$ is the linear, back-transformed biomass in a compartment of a single tree, and RMSE_j is the root mean square error (average residual) of the relevant $\ln(W_{j,\,k})$ (Table 3). For each of the tree compartments, the total biomass within a plot for a given year, $W_{j,\,p}$ (kg ha^{-1}), was obtained by adding together the individual trees in the net plot examined and dividing by the area of the latter. On average, 35 trees (range 26–42) were examined per net plot before the thinning in 1993, and 121 trees (range 103–115) in the extended net plot used after it. For stumps and roots, a general allometric regression for several tree species developed by Petersson

Table 3
Allometric functions used to estimate the biomass of different compartments of a single tree as a function of chest-height stem diameter.

Component	Regression	RMSE(ln(W_j))	$u_{rel,\ allometric}(W_j)$, before 1993 thinning[a]	$u_{rel,\ allometric}(W_j)$, after 1993 thinning[b]
Stem (wood + bark)	$\ln(W) = -2.541 + 2.367\ln(D)$[c]	0.1483[d]	1.5%	0.76%
Needles	$\ln(W) = -3.335 + 2.032\ln(D)$[c]	0.2928[d]	2.9%	1.5%
Living branches	$\ln(W) = -3.988 + 2.284\ln(D)$[c]	0.2990[d]	3.1%	1.6%
Dead branches	$\ln(W) = -4.541 + 2.214\ln(D)$[c]	0.4312[d]	4.5%	2.2%
Stumps and roots	$\ln(W) = 4.52965 + 10.57571 \times (D/(D + 142))$[e]	0.31487[e]	3.3%	1.6%

[a] Relative standard uncertainty for estimating average biomasses over the four plots, based on 26–42 trees measured per plot before the thinning performed in 1993.
[b] Ditto, based on 103–115 trees per plot after the thinning performed in 1993.
[c] Regression obtained from Ågren et al. (personal communication); W is dry weight in kg and D is chest-height stem diameter in cm.
[d] Root mean square error of regression, on a logarithmic scale, based on data obtained from the authors of Ågren et al. (personal communication).
[e] Regression and RMSE from Petersson and Ståhl (2006); W is dry weight in g and D is chest-height diameter in mm.

and Ståhl (2006) was used (Table 3). For above-ground compartments, the allometric functions in Table 3 had been developed by Ågren et al. (personal communication) based on 324 trees felled on four occasions (1987, 1990, 1993 and 2001) in the present field experiment. There were no significant differences between treatments in these functions, so data from all the treatments form the basis for the above-ground regressions in Table 3. It was furthermore found that including tree height or the lower boundary of the canopy in the regressions changed the predictions to a very small extent and in some cases yielded greater prediction errors. Among the tree compartments mentioned above, the dry weights of stem bark (W_{Bark}) and stem wood (W_{Wood}) were calculated collectively by one common allometric function for the dry weight of stem (W_{Stem}; Table 3), which had to be separated using year-specific bark-to-stem ratios (Bark/Stem):

$$W_{Bark} = (Bark/Stem) \times W_{Stem} \quad (16)$$

$$W_{Wood} = [1 - (Bark/Stem)] \times W_{Stem} \quad (17)$$

Generalised (year-specific but common for all plots) bark-to-stem ratios were established for trees felled in the investigated control plots in 1987, 1990 and 2001; for 1993, a ratio was obtained by linear interpolation.

With a few exceptions, as described in Section 2.6.2, base cation concentrations in above-ground tree tissues (stem wood, stem bark, needles, living branches and dead branches) from each plot, $Conc_{i,\ j,\ p}$, were obtained by analysing samples from two to three evenly distributed and representative trees felled in each plot in 1987, 1993 and 2001. Samples were analysed using ICP-ES after digestion in concentrated HNO_3 and $HClO_4$ (volume-to-volume ratio of the acids, 10:1). Neglecting any bioaccumulation of Na, a concentration of the base cation equivalent sum, $Conc_{\Sigma BC,\ j,\ p}$ ($mol_c\ kg^{-1}$), was calculated based on the concentrations of Ca, Mg and K.

For the stump and root compartment ('Stump-root' in the equations below), it was assumed that the concentration of a given cation in a given year equalled the mass-weighted average concentration in stem wood and stem bark according to Eq. (18):

$$Conc_{i,\ Stump\text{-}root,\ p} = (Bark/Stem) \times Conc_{i,\ Bark,\ p} + [1 - (Bark/Stem)] \times Conc_{i,\ Wood,\ p} \quad (18)$$

It follows that to calculate the pool of a given cation for a given year, Eq. (14a) could be applied directly for the compartments of needles, living branches and dead branches. The pools in stem bark and stem wood ($Pool_{i,\ Bark,\ p}$ and $Pool_{i,\ Wood,\ p}$) were calculated using Eqs. (14b) and (14c), respectively:

$$Pool_{i,\ Bark,\ p} = (Bark/Stem) \times W_{Stem,\ p} \times Conc_{i,\ Bark,\ p} \quad (14b)$$

$$Pool_{i,\ Wood,\ p} = [1 - (Bark/Stem)] \times W_{Stem,\ p} \times Conc_{i,\ Wood,\ p} \quad (14c)$$

Finally, plot-wise cation pools in stumps and roots ($Pool_{i,\ Stump\text{-}root,\ p}$) were calculated using Eq. (14d):

$$Pool_{i,\ Stump\text{-}root,\ p} = W_{Stump\text{-}root,\ p} \times [(Bark/Stem) \times Conc_{i,\ Bark,\ p} + [1 - (Bark/Stem)] \times Conc_{i,\ Wood,\ p}] \quad (14d)$$

Eqs. (14a)–(14d) yielded year-specific values of the '$Pool_{i,\ j,\ p}$' terms of Eq. (13).

2.6.2. Combined standard uncertainty of the rate of bioaccumulation

Over the four plots, an average accumulation of each cation in the biomass, $Bioacc_i$, and a combined standard uncertainty, $u_c(Bioacc_i)$, were calculated. Due to the complex nature of Eq. (13) and the underlying Eqs. (14)–(18), no attempt was made to develop an analytical expression for the combined standard uncertainty. Instead, the aforementioned spreadsheet solution was used to quantify the change in $Bioacc_i$ when each of the variables in the calculation was changed one standard uncertainty away from its nominal value. The sum of squares in $Bioacc_i$ (one squared change per shifted variable) was equivalent to the squared combined standard uncertainty in $Bioacc_i$. The square root of this yielded the combined standard uncertainty of $Bioacc_i$. Due to incomplete plot-wise data, this was done using average values over the four plots for the variables in Eqs. (14)–(18), and the standard errors and standard uncertainties listed in Table 2. The latter are described in the remainder of this section.

For biomass in each compartment, a Type A standard error accounting for spatial variability over the four control plots was calculated from the standard deviation over the four plots; expressed as a percentage of the mean, it ranged from 6% to 11%. This relative standard error was basically the between-plot variability of calliper measurements at biomass scale. It is referred to as a year-specific '$SE_{rel}(W_j)$' in Table 2. The error in stem diameter measurements was shown to be negligible in biomass determinations by Yanai et al. (2010), and was not considered here.

For the allometric functions, a relative Type B standard uncertainty for each tree compartment, $u_{rel,\ allometric}(W_j)$, was assessed using a Monte Carlo procedure based on individual tree diameters and the RMSE-values of Table 3. For each sampling occasion (1987, 1993 and 2001), it was calculated as the relative standard deviation over 1000 realisations of the average-plot biomass, W_j ($kg\ ha^{-1}$). In the procedure, the expected prediction error for the log biomass of a biomass compartment ('j') in a single tree ('k'), $u(\ln(W_{j,\ k}))$, was first calculated as a function of tree diameter, D, according to conventional theory of linear regression:

$$u(\ln(W_{j,\ k})) = \left[RMSE_j^2 \times \left(1 + \frac{1}{n_{cal}} + \frac{\left[\ln(D_k) - \overline{\ln(D)_{cal}}\right]^2}{SS(\ln(D))_{cal}} \right) \right]^{1/2}. \quad (19)$$

The number n_{cal} are the 324 trees of the calibration data set; D_k is the diameter of the tree whose biomass is going to be predicted; $\overline{\ln(D)}_{cal}$ and $SS(\ln(D))_{cal}$ are the mean and sum of squares of log diameters in the calibration data set, respectively. The factor by which $RMSE_j^2$ was multiplied in Eq. (19) ranged from 1.00 to 1.09 with an average of 1.01. Given the lack of access to calibration data for the allometric function of stumps and roots according to Petersson and Ståhl (2006), the relevant $RMSE^2$ was used uncorrected for this tree compartment. To each individual $\ln(W_{j,k})$ noise was added that was $u(\ln(W_{j,k}))$ multiplied by a normally distributed random number that had a mean of zero and standard deviation of one. The resulting distorted values of $\ln(W_{j,k})$ were then back-transformed, using Eq. (15), into the biomasses for individual trees, $W_{j,k}$. The latter were added together for all the trees examined in the four net plots, and divided by their combined area to yield the average plot areal biomass (kg ha^{-1}), W_j. Each of the 1000 realisations was calculated with a new set of randomly distorted $\ln(W_{j,k})$. It can be seen in Table 3 that $u_{rel,\ allometric}(W_j)$ became smaller owing to the larger number of observations in the extended net plots after the thinning in 1993.

To account for both Type A and B uncertainties in the spreadsheet solution, all biomasses for a given year, W_j in Eqs. (14a)–(14d), were multiplied by two factors, each with the nominal value of one, and the standard deviation of $SE_{rel}(W_j)$ and $u_{rel,\ allometric}(W_j)$, respectively. Also, the bark-to-stem ratio present in Eqs. (14b)–(14d) was given Type B uncertainty, because partly interpolated average plot values were used. Thus, the ratio was multiplied by a factor having the nominal value of one and the standard uncertainty of u_{rel}(Bark/Stem), which was estimated at 4.4% from available data.

For base cation concentrations, 'Type A' relative standard errors over the plots were calculated for Ca, Mg, K and their equivalent sum in stem wood, stem bark, needles, living branches and dead branches. In the spreadsheet solution, all average concentrations, $Conc_{i,j}$, used in Eqs. (14a)–(14d) were multiplied by a factor having the nominal value of one and the standard uncertainty $SE_{rel}(Conc_{i,j})$, as relevant for the year of interest. For 2001, standard errors were available for all these above-ground compartments. However, plot-wise concentrations were unavailable from 1987 for all compartments, and for the stem compartments in 1993. Therefore, for stem compartments standard errors from 2001 were used for 1987 and 1993 as well. For the remaining above-ground compartments (needles, living branches and dead branches) standard errors from 1993 were used also for 1987. All standard errors for concentrations, $SE_{rel}(Conc_{i,j})$, were considered as Type A uncertainties, whether they were obtained from the year of interest or inferred from other samplings. They were highly variable and ranged from 0.4% to 23% for Ca, Mg, K and their equivalent sum.

Finally, the assumption that the concentration of a cation in stumps and roots equalled the mass weighted average of the concentration in stem bark and stem wood was ascribed a guesstimated 'Type B' relative standard uncertainty, u_{rel}(Stump-root conc), of 10%. To take this uncertainty into account, each $Pool_{i,\ Stump\text{-}root}$ from Eq. (14d) was multiplied by a common factor having the nominal value of one and the standard uncertainty of 0.1. The factor accounted for a systematic error in the assumption, in addition to the variability already taken into account via the above-ground compartments.

When calculating $u_c(Bioacc_i)$ using the spreadsheet solution, an underlying assumption was that the variables contributing to $Bioacc_i$ were independent. This was justified by the general absence of significant correlations between biomass change and cation concentrations in the present material. It can be seen that some variables appeared several times in Eq. (13) and the underlying Eqs. (14)–(18). An important feature of the spreadsheet solution was that all these equations were calculated simultaneously. Therefore, each variable was shifted in all pertinent equations simultaneously, and yielded only one single contribution to the sum of squares constituting $(u_c(Bioacc_i))^2$. This prevented multiple manifestations of one single uncertainty from fraudulently propagating as if they were independent errors.

When estimating $u_c(Bioacc_i)$ based on average plot calculations as described above, it was possible to circumvent the missing plot-wise concentrations for some tree compartments. When performing the Monte Carlo calculation of weathering rates according to Eq. (1b), however, complete plot-wise data were critical and missing plot-wise concentrations had to be re-constructed by adding noise to the available plot means. The added noise was the relevant standard deviation over plots, as available from 1993 or 2001, multiplied by a normally distributed random number that had a mean of zero and standard deviation of one. In a larger data set, one is likely to find significant correlations between tree size and cation concentrations in tree tissues (Rothpfeffer and Karltun, 2007). However, the current data did not show consistent correlations between biomasses and concentrations. By consequence, cation concentrations of individual plots and on individual sampling occasions were treated as independent random variables in this procedure.

2.7. Internal cycling: gross uptake, canopy excretion and litter fall

In addition to the net fluxes that constitute the terms of the weathering budget, Eq. (1), the internal fluxes of the elements Ca, Mg and K were quantified. Gross uptake rates of Ca, Mg and K ($Gross\ uptake_i$) were calculated from the rates of bioaccumulation ($Bioacc_i$), litter fall ($Litter_i$) and canopy excretion ($Excret_i$), all having the unit of kg ha^{-1} yr^{-1}:

$$Gross\ uptake_i = Bioacc_i + Litter_i + Excret_i \quad (20)$$

The bioaccumulation term is described in Section 2.6.1. The litter fluxes of base cations were measured during 1989–1997 by analysing needles that had fallen onto nylon mesh litterfall collectors (9 collectors per plot, 0.25 m^2 each, emptied 4–11 times per year). Base cation concentrations in the needle litter (approximately 90% of the total litter in the control plots) were analysed using ICP-ES after digestion in concentrated HNO_3 and $HClO_4$ (ratio 10:1). The term '$Litter_i$' in Eq. (20) is the grand annual mean over the four plots.

The canopy excretion of a cation, $Excret_i$, was calculated as the difference between throughfall (TF_i) and deposition (Dep_i), both described in Section 2.3 above. Using Eq. (2), this produces the following equation:

$$Excret_i = TF_i - Dep_i = TF_i - OF_i \times \frac{TF_{Na}}{OF_{Na}} \quad (21)$$

Only average plot data were available for litterfall, and the terms of throughfall and deposition in Eq. (20) are likely to be dependent on one another. Therefore, only central values were calculated for gross uptake and canopy excretion.

3. Results

3.1. Weathering rates and overall cation cycling

Fig. 1 shows average fluxes for the base cations along with average pools during the study period. The rapid turnover of exchangeable cations and the small magnitude of weathering compared to the overall cycling of cations in the system are striking. The geochemical pools in this and similar boreal ecosystems are very large compared to all the other pools and fluxes. The yearly production of above-ground biomass (data from this paper) and needle litter (data from Nilsson et al., 2001) during the study period were fairly constant at approximately 5 and 2 ton ha^{-1} yr^{-1} of dry matter,

respectively (Fig. 2). In the beginning of the period, the aboveground biomass was 90 ton ha^{-1} dry weight on average; at the end it was 154 ton ha^{-1}.

Central values for weathering rates according to cation budgets indicated a net release of 2.4, 1.4, 0.3 and 2.3 kg ha^{-1} yr^{-1} for Ca, Mg, K and Na respectively (Table 4). Confidence intervals were obtained by multiplying the combined standard uncertainties by 3.18, which corresponds to the *t*-value for 3 degrees of freedom (4 replicates) at the 95% level. The amplitude of these intervals was similar to (Mg) or larger than (Ca, K and Na) the nominal weathering rates themselves. Accordingly, most cations had weathering rates that were not significantly separated from zero. However, nominal (central) values for individual plots in Table 4 were consistently positive for Mg and Na, whereas negative excursions occurred for Ca and K.

For Ca and K, Type A uncertainties accounted for almost all (>90%) of the extended SE, whereas for Mg and Na Type B uncertainties were prominent (Table 4). This is due to the way different terms dominated the budget of the different cations, and the preponderance of Type A or B uncertainties in the different budget terms (shown in Section 3.2 below). Particularly for Ca and K, the relative contributions to the extended standard errors (Table 4) indicated that bioaccumulation was important, both as a term in the cation budget and as a source of uncertainty. Deposition and leaching had a large influence on Mg and Na due to the high deposition of sea salts at the particular study site. The change in exchangeable cations appeared to be of little importance for uncertainties in weathering rates for all base cations.

3.2. Individual terms of cation budgets

3.2.1. Rate of deposition

Table 5 shows mean values and standard uncertainties for the deposition of base cations in the experiment. The deposition of Ca, Mg and K was in the range 3–4 kg ha^{-1} yr^{-1}. Na had a much larger input, approximately 30 kg ha yr^{-1}. The combined standard uncertainties were essentially a result of the between-plot standard error of TF_{Na}, and of covariances involving this flux. The contributions from the different $u_{rel}(OF_i)$ were small in themselves, but propagated via the covariances of OF_i with TF_{Na}. With the different $u_{rel}(OF_i)$, including $u_{rel}(OF_{Na})$, set to zero, the combined standard uncertainty of deposition became identical to the Type A standard error, $SE(Dep_i)$. In terms of weathering rate, ignoring the Type B uncertainties affected only Mg noticeably, by yielding a slightly underestimated extended standard error, $SE_{extended}(Weath_{Mg})$, of 0.32 instead of from 0.44 kg ha^{-1} yr^{-1}.

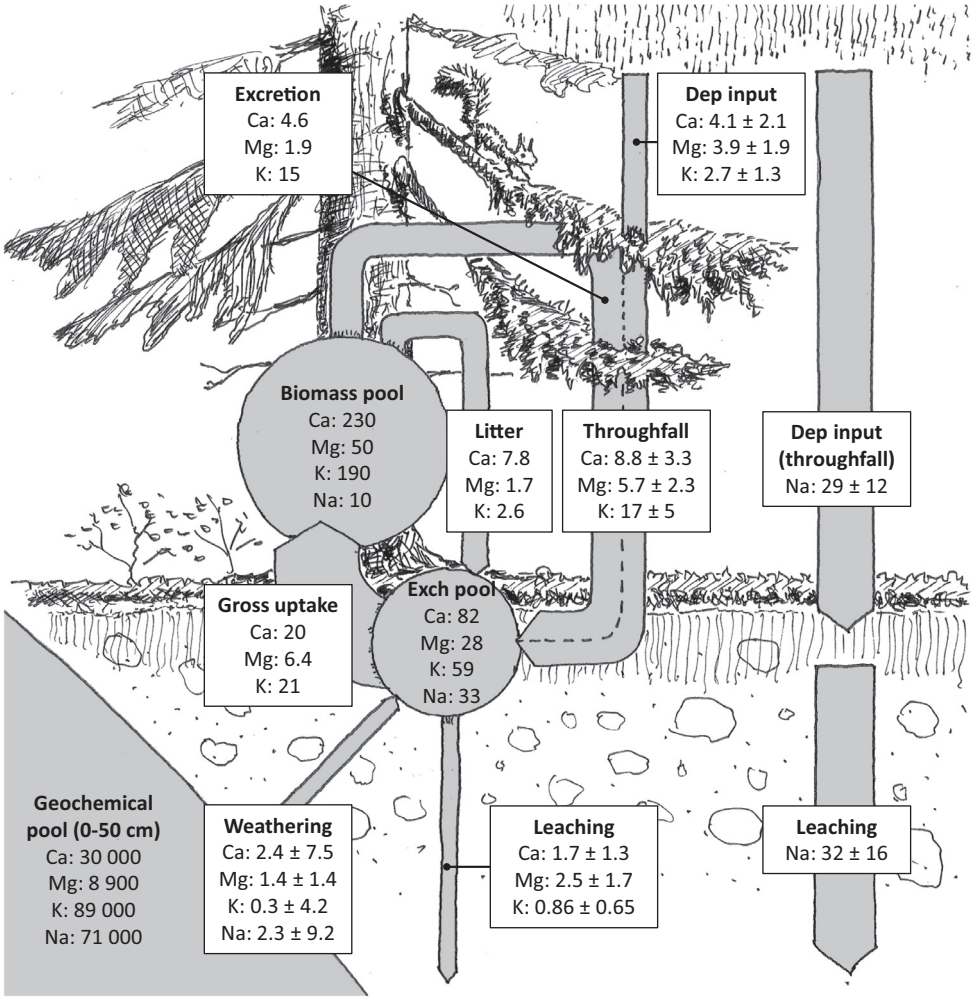

Fig. 1. Average pools (circles, kg ha^{-1}) and fluxes (arrows with white plates, kg ha^{-1} yr^{-1}) of Ca, Mg, K and Na during 1987–2001 in the experimental forest at Skogaby, southwest Sweden. Circle areas and arrow widths are proportional to the equivalent sum of the cations included. Soil pools are calculated for 0–50 cm depth, and most of the area representing the geochemical pool is outside the figure. Where shown, confidence intervals were calculated based on the extended standard error (weathering), ordinary standard errors (throughfall of Na) or combined standard uncertainties (remaining cation budget terms) and a *t*-value of 3.18 (the 95-% level, 3 degrees of freedom). Geochemical composition of the fine earth was measured using ICP-MS after fusion with $LiBO_2$ and dissolution in HNO_3; conversion to kg ha^{-1} values done similarly as for exchangeable cations. Rounded figures for 'gross uptake' and 'excretion' make some of these fluxes apparently in conflict with data in the relevant tables.

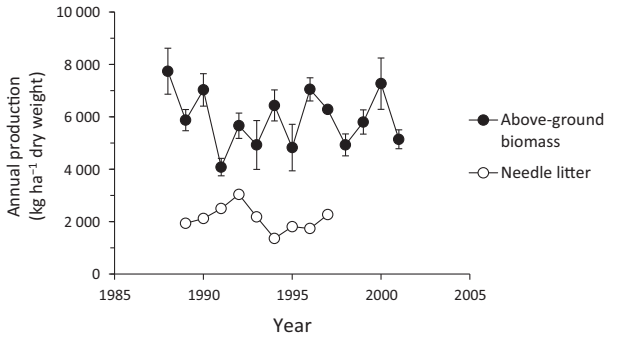

Fig. 2. Annual production in above-ground biomass (annual increment of standing biomass) and annual needle litter fall: mean over the four control plots. Error bars indicate standard errors for the biomass ('Type A' uncertainty); only mean over all control plots were available for the litter.

3.2.2. Rate of change in exchangeable base cations

Confidence intervals based on the *t*-value of 3.18 suggested a significant decline of exchangeable Ca, K and ΣBC, and more or less stationary pools of exchangeable Mg and Na (Table 6), at least during the later years of the study period (Fig. 3). The decline of exchangeable Ca and K may to some extent be associated with a slight degradation of the forest floor, as suggested by the decrease over time of the FH-layer mass in Fig. 3a (regression on year close to significant, $P = 0.055$). For K and ΣBC processes in the mineral soil ('0–50 cm' in Fig. 3) were important for the evolution of exchangeable pools.

The relative contributions to the combined standard uncertainty were dominated by Type A uncertainties. Type B uncertainties of dry bulk density and of the content of stones and boulders were of lesser importance (Table 6). This is not to say that dry bulk density and stoniness were not critical, but that the variability of plot-wise performed measurements dominated over the systematic error in stoniness and the error in generalised bulk densities. Uncertainties in the estimated cation content of the L-layer in early years showed to be somewhat important for the divalent cations of Ca and Mg, whereas exchangeable K and Na were predominantly found in the mineral soil (0–50 cm, Fig. 3) and appeared little affected by this uncertainty.

Fig. 3 shows abrupt increases and decreases in the pools of exchangeable cations, notably during early years. These changes, in the range of 10–20 kg ha^{-1} over only a few years, were of a similar order of magnitude as the annual gross uptake (Ca, Mg and K) or deposition (Na) presented in Fig. 1.

3.2.3. Rate of leaching

The concentrations of base cations in soil solutions at 50 cm depth varied considerably between plots and between sampling occasions (Fig. 4). Modelled water fluxes showed long periods with only small water movement, interrupted by peaks with high rates of vertical flow. Typically, as much as 90% of the water runoff occurred during approximately 25% of the time. The data did not reveal any significant correlation between water flow rates and cation concentrations, and the calculated leaching appeared to be strongly dependent on the modelled runoff of water. Temporal variability was greater than spatial variability: Relative standard deviations between years of calculated cation fluxes in single plots were in the range of 33–83% (not shown), to be compared with the relative standard errors due to between-plot variability in measured concentrations, $SE_{rel}(Conc_i)$, which were 3–19% (Table 2).

Deposition and leaching of chloride indicated considerable mismatch between the estimates of the two fluxes. As shown in Fig. 5, the pattern was similar for the uncorrected flux of Na, indicating that there was indeed a bias in estimated deposition and/or leaching, due to circumstances that were different for each plot. The correction ratio of Eq. (11) ranged from 0.77 to 1.97 for the four plots. The corrected leaching losses were in the range of 0.86–2.5 kg ha^{-1} yr^{-1} (central values) for Ca, Mg and K. For Na, it was considerably greater due to the marine influence at the site (Table 7). The guesstimated 10% relative standard uncertainty of modelled water flux, u_{rel}(Flux), was highly critical for the uncertainty in the weathering rate for Na and to some extent for Mg. Eliminating u_{rel}(Flux) by setting it to 0 % yielded an extended SE of weathering that was only 0.32 and 0.51 kg ha^{-1} yr^{-1} for Mg and Na. With a u_{rel}(Flux) of 20%, the extended SE became 0.6 and 6 kg ha^{-1} yr^{-1} for Mg and Na, respectively.

3.2.4. Rate of bioaccumulation

Concentrations of Ca and K in tree tissues showed a decline over time, as expected for a young to middle-aged tree stand, whereas the concentration of Mg was more or less constant (not shown). The mean base cation accumulation in tree biomass was 7.4, 2.8 and 4.2 kg ha^{-1} yr^{-1} for Ca, Mg and K respectively (Table 8). Of

Table 4
Rates of base cation weathering (kg ha^{-1} yr^{-1}), expressed as a mean over the four investigated plots, and the range of nominal values obtained from the individual plots. Also shown is the extended standard error of the mean, $SE_{extended}(Weath_i)$. 'Type A only' is the standard error of the mean for the four plots, when Type B uncertainties were switched off in the Monte Carlo calculation; 'Type B additional…' is the remaining part of the extended standard error (the sum of the squared contributions is equal to the squared $SE_{extended}(Weath_i)$, rounded values). In addition, the relative contributions (percentages) to the extended SE are divided in two different ways: into Type A and B uncertainties collectively, and into the contributions from different terms in the cation budget. The confidence intervals were calculated based on the extended standard error and a *t*-value of 3.18 (the 95-% level, 3 degrees of freedom).

Statistics and contributions	Ca (kg ha^{-1} yr^{-1}) or %	Mg	K	Na	ΣBC (kmol$_c$ ha^{-1} yr^{-1}) or %
Mean, four plots	2.4	1.4	0.3	2.3	0.33
Range, individual plots, no noise added	−2.9 to 6.1	0.8 to 1.9	−2.2 to 3.3	0.9 to 3.2	0.01 to 0.62
Extended standard error, $SE_{extended}(Weath_i)$	2.4	0.44	1.3	2.9	0.27
Type A only, $SE(Weath_i)$	2.3	0.23	1.3	0.51	0.14
Type B additional uncertainty	0.6	0.38	0.28	2.8	0.23
Confidence interval (95%), Type A and B uncertainties	±7.5	±1.4	±4.2	±9.2	±0.85
Relative contributions to the extended SE, Type and B uncertainties collectively					
Type A	95%	27%	96%	3%	28%
Type B	5%	73%	4%	97%	72%
Relative contributions to the extended SE, different terms of the cation budget					
Deposition and Leaching (two strongly interdependent terms together)	6%	81%	4%	106%	73%
Change in exchangeable cations	2%	2%	4%	1%	1%
Accumulation in biomass	79%	20%	82%	0%	25%
Covariances, in addition to Deposition and Leaching	14%	−3%	10%	−7%	2%

Table 5
Mean and combined standard uncertainty, $u_c(Dep_i)$, of the rates of deposition of base cations. 'Type A only' is the standard error over the four plots, when Type B uncertainties were ignored; 'Type B' is the part of the combined standard uncertainty that derived from Type B uncertainties (cf. Table 2). Also shown are the relative contributions (%) to $u_c(Dep_i)$; see Eq. (6). Confidence intervals for the deposition rates are provided in Fig. 1.

Statistics and contributions	Ca (kg ha^{-1} yr^{-1}) or %	Mg	K	Na	Cl	ΣBC (kmol$_c$ ha^{-1} yr^{-1}) or %
Mean	4.1	3.9	2.7	29	54	1.9
Combined standard uncertainty, $u_c(Dep_i)$	0.65	0.61	0.41	3.7	8.7	0.30
Type A only, SE(Dep_i)	0.51	0.48	0.33	3.7	6.8	0.23
Type B additional uncertainty, $u_{Type\ B}(Dep_i)$	0.40	0.37	0.24	NA[a]	5.5	0.19
Relative contributions to $u_c(Dep_i)$						
Type A: Throughfall of Na, $SE_{rel}(TF_{Na})$	62%	63%	65%	100%	60%	61%
Type B: Open-field dep., ion of interest, $u_{rel}(OF_i)$	2%	2%	1%	NA[a]	2%	2%
Type B: Open-field dep., Na, $u_{rel}(OF_{Na})$	2%	2%	2%	NA[a]	2%	2%
Type B: Covariance (TF_{Na}, OF_i)	12%	11%	9%	NA[a]	15%	14%
Type B: Covariance (TF_{Na}, OF_{Na})	19%	19%	20%	NA[a]	18%	18%
Type B: Covariance, (OF_i, OF_{Na})	3%	3%	2%	NA[a]	4%	3%

[a] Not applicable.

Table 6
Mean and combined standard uncertainty, $u_c(\Delta Exch_i)$, of the rates of change in exchangeable base cations. 'Type A only' is the standard error over the four plots, if Type B uncertainties were ignored; 'Type B' is the part of the combined standard uncertainty that derived from Type B uncertainties (cf. Table 2). Relative contributions (%) to $u_c(\Delta Exch_i)$ were calculated in analogy with Eq. (6). Confidence intervals were calculated based on the combined standard uncertainty and a *t*-value of 3.18 (the 95-% level, 3 degrees of freedom).

Statistics and contributions	Ca (kg ha^{-1} yr^{-1}) or %	Mg	K	Na	ΣBC (kmol$_c$ ha^{-1} yr^{-1}) or %
Mean change, four plots	−2.7	−0.02	−2.1	−0.76	−0.22
Combined standard uncertainty, $u_c(\Delta Exch_i)$	0.32	0.06	0.27	0.26	0.02
Type A only, SE($\Delta Exch_i$)	0.28	0.05	0.25	0.25	0.02
Type B additional uncertainty, $u_{Type\ B}(\Delta Exch_i)$	0.16	0.03	0.08	0.07	0.01
Confidence interval (95%), Type A and B uncertainties	±1.0	±0.19	±0.8	±0.83	±0.08
Relative contributions to $u_c(\Delta Exch_i)$					
Type A: Between-plot variability, SE($\Delta Exch_i$)	74%	74%	90%	94%	66%
Type B: Cations in litter (L) layer early years	15%	17%	4%	0.1%	15%
Type B: Dry bulk density	7%	6%	5%	4%	10%
Type B: Stones and boulders	5%	2%	1%	3%	8%

the individual contributions to the combined standard uncertainty, it can be seen in Table 8 that Type A uncertainties in biomass and concentrations dominated for all cations. The uncertainties in allometric functions, which were considerable for a single tree, were of little importance when estimating the biomass over several plots. This is on condition that biases in addition to the RMSE-values of the allometric functions were absent. Errors in the ratio of Bark/Stem contributed only little uncertainty. Also, the guesstimated 10% systematic error in the assumption about cation concentrations in the stump and root compartment was of minor importance; the calculation was not particularly sensitive to a shift in this value. Tentatively increasing u_{rel}(Stump-root conc) to 50% yielded a combined standard uncertainty, u_c(Bioacc$_i$), of 1.8, 0.41 and 1.4 (kg ha^{-1} yr^{-1}) for Ca, Mg and K, and 0.15 for their equivalent sum.

4. Discussion

4.1. Characteristics of the base cation fluxes

The nominal weathering estimates in Table 4 were comparable to the results of Olsson and Melkerud (2000), who reported annual base cation weathering rates of 0.6–2.7 kg ha^{-1} yr^{-1} for three Nordic forest soils since the last deglaciation. The cations differed regarding their pools and fluxes. For Ca, accumulation in the biomass potentially constituted the largest term in the cation budget (7.4 ± 5.4 ha^{-1} yr^{-1}; Table 8) besides deposition (4.1 ± 2.1 kg ha^{-1} yr^{-1}; Fig. 1). Although the confidence intervals suggest some uncertainty as to whether there was a deficit in weathering rate (2.4 ± 7.5 ha^{-1} yr^{-1}) compared to the accumulation in the biomass, exchangeable Ca in the soil showed a declining trend (Table 6; Fig. 3), and would be even more so with less Ca deposition. The importance of atmospheric deposition for the cycling of Ca in forest stands has been elucidated in numerous studies (e.g., Bélanger and Holmden, 2010). Deposition may provide the majority of Ca taken up by trees, depending on conditions for soil weathering and deposition. It was found to contribute almost 100 % of the Ca taken up in a setting with a large marine influence in the northwest USA (Perakis et al., 2006).

The budget of K resembled that of Ca in many ways: The accumulation rate in the biomass was potentially high (4.2 ± 4.3 kg ha^{-1} yr^{-1}; Table 8), the weathering rate was highly uncertain (0.3 ± 4.2 kg ha^{-1} yr^{-1}) and there was a negative change in exchangeable K in the soil (−2.1 ± 0.8 kg ha^{-1} yr^{-1}; Table 6). The deposition input (2.7 ± 1.3 kg ha^{-1} yr^{-1}; Fig. 1) appeared substantial, although its confidence interval had an overlap with that of leaching (0.86 ± 0.65 kg ha^{-1} yr^{-1}; Table 7).

For Mg, leaching (2.5 ± 1.7 kg ha^{-1} yr^{-1}; Fig. 1) and accumulation in the biomass (2.8 ± 1.1 kg ha^{-1} yr^{-1}; Table 8) were similarly important sinks. The weathering rate was 1.4 ± 1.4 kg ha^{-1} yr^{-1} (Table 4), and the input from deposition 3.9 ± 1.9 kg ha^{-1} yr^{-1} (Fig. 1). Deposition of Mg therefore appeared important to prevent a decline in the pool of the exchangeable Mg in the soil (Table 6).

For Na the deposition was large, owing to the extensive marine inputs at this site. The accumulation of Na in the biomass was not

estimated due to the lack of early period data. However, the pool of Na in above-ground biomass was 10 kg ha^{-1} on average for available data (Fig. 1). Assuming approximately constant Na concentrations in tree tissues over time, the typical annual increment of the biomass suggests a bioaccumulation of Na of about 0.3 kg ha^{-1} yr^{-1}, which is negligible in the context of its cation budget. In the absence of significant changes in the pool of exchangeable Na (Table 6), the deposition input was most probably balanced by leaching. Hence, the large uncertainties in deposition and leaching cannot be considered as independent errors.

4.2. The difficulty of assessing small weathering rates from cation budgets

According to Table 4, it is clearly difficult to measure with sufficient accuracy the small weathering rates that prevail in the rather slowly weathering soils of many forest ecosystems. For ΣBC, the range of nominal (central) values of individual plots (0.01–0.62 $kmol_c$ ha^{-1} yr^{-1}) was somewhat narrower, and the confidence interval (0.33 ± 0.85 $kmol_c$ ha^{-1} yr^{-1}) somewhat wider, than the range of weathering rates estimated by Hodson and Langan (1999) for a Scotish till of granitic origin. Compared to the range of weathering rates of Ca and K, estimated by Klaminder et al. (2011) for at granitic setting in northern Sweden using various methods, our confidence intervals have amplitudes similar to those delimited by their judiciously assessed upper and lower constraints for the weathering rates.

The need for replicates to obtain realistic estimates is obvious (Table 4). Weathering in this study turned out to be a small flux in the overall element cycles, making it an inherently difficult variable to assess. Gross uptake rates were several times greater than the central values of weathering rates (Fig. 1). The study site has relatively small pools of exchangeable base cations, and is situated in a region in southwest Sweden with an expected high rate of

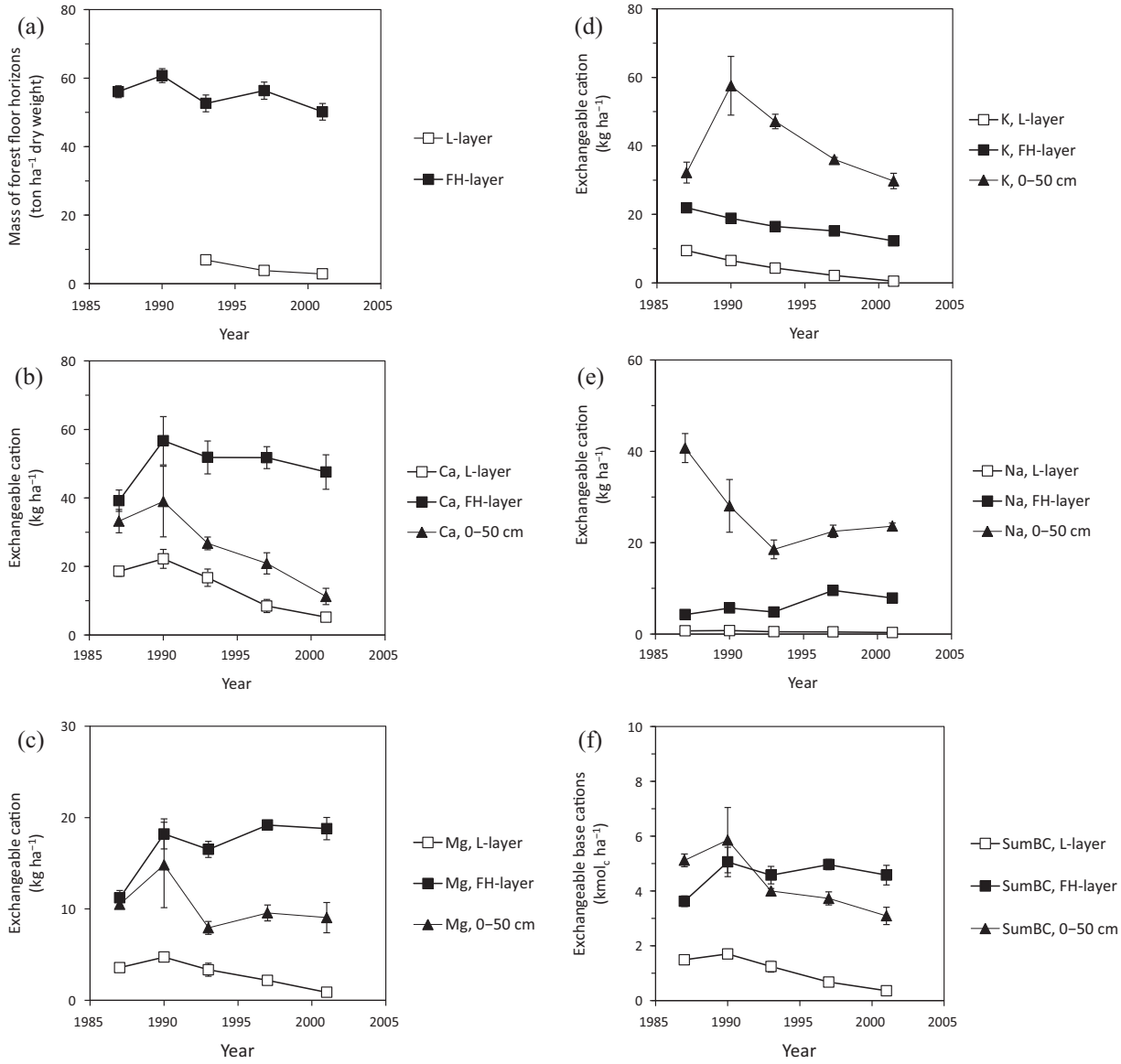

Fig. 3. Temporal trends of (a) dry matter in the forest floor (litter, 'L-layer', and humus, 'FH-layer'), (b–e) individual exchangeable base cations in forest floor and mineral soil (0–50 cm depth) and (f) the sum of exchangeable base cations. Dots represent means over the four control plots of the experiment, error bars show the standard error over these plots ('Type A' uncertainty only). The L-layer in (a) was not measured in 1987 and 1990, but its cation content in (b–f) was estimated from the ratio of L/FH, in terms of cation content, obtained in later years (see Section 2.4).

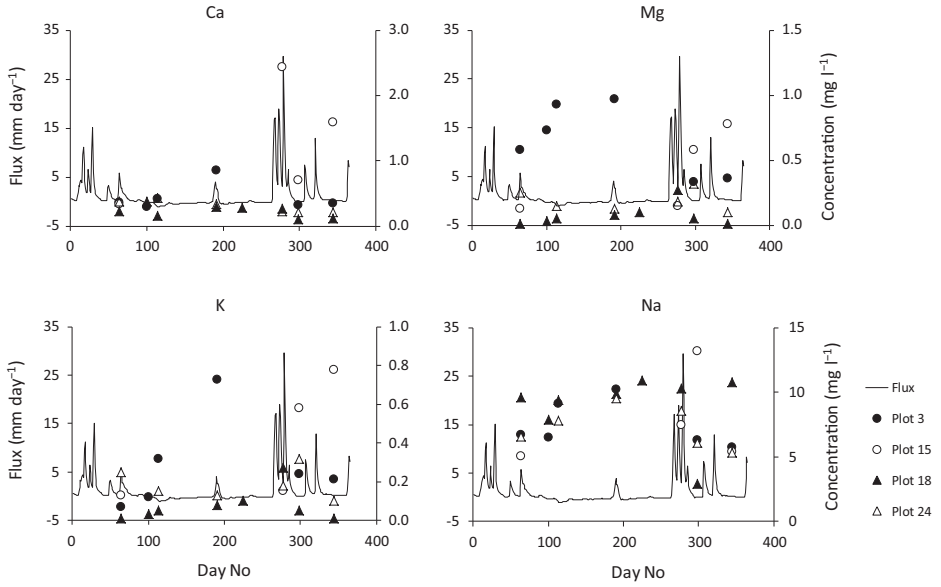

Fig. 4. For a sample year, 1990, daily simulated vertical water flux at 50 cm depth (mm day^{-1}, one generalised daily flux for all plots) and measured base cation concentrations of individual plots on a maximum of eight sampling occasions.

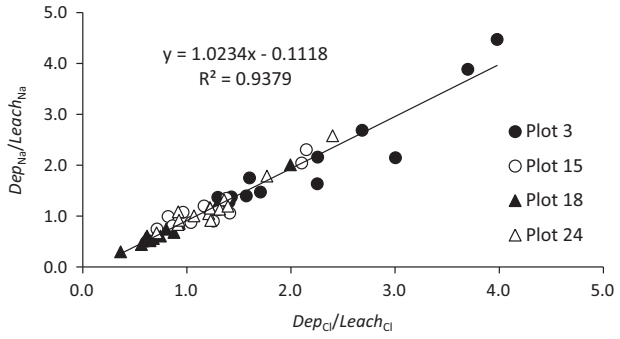

Fig. 5. Ratios of deposition over leaching for Cl vs. the same ratio for Na (the latter before correction for mismatch between deposition and leaching). Each data point for a plot represents the ratio of cumulative fluxes (kg ha^{-1} yr^{-1}) from an individual year during 1989–2001. Deviations from the value one for Cl indicates bias in the estimate of leaching compared to deposition if this element. The similar pattern for Na suggests systematic mismatch due to plot-specific circumstances (regression line for all plots collectively).

accumulation of N in the forest ecosystem (Akselsson et al., 2007). A concomitant high demand for base cations from weathering may therefore be expected. It is noteworthy that, despite this, exploitation of weatherable soil minerals was a subordinate feature in the cycling of base cations. The confidence intervals of weathering rates had amplitudes larger than the nominal estimates themselves, and for most elements extended below zero. Potentially negative weathering was also obtained by Klaminder et al. (2011) for Ca. When calculating element budgets for potassium in agricultural systems, similarly uncertain weathering rates were obtained in soils where the weathering was slow due to a coarse soil texture. In contrast, soils with a high weathering potential showed weathering rates that were significantly different from zero (Simonsson et al., 2007), suggesting that a threshold in the weathering rate had to be overcome for conclusions to be drawn about its absolute magnitude or even whether it was positive or negative.

The question arises what is a realistic range of values calculated by Eq. (1b), especially whether it may comprise negative values. As pointed out in Section 2.2.1, the calculated 'weathering' in this study may comprehend any mobilisation from or accumulation in soil pools other than the exchange complex above 50 cm depth in the soil. For Ca, these processes may include build-up or slow release of non-exchangeable cation associated with litter in the forest floor. The release of such Ca during decomposition of forest litter may take a couple of years (Likens et al., 1998). Furthermore, fluxes between the soil solution and an oxalate reserve may be important for Ca, as suggested by Bailey et al. (2003). Therefore, negative 'weathering' of Ca is not obviously unrealistic. The other base cations are more readily released during litter decomposition (Berg and Staaf, 1980). For K, negative weathering is compatible with fixation in clay minerals. Mineralogical evidence for fixation of K in the root zone, even during the growth season, was found in a forest ecosystem by Turpault et al. (2008) and Calvaruso et al. (2009). However, at Skogaby the decline in exchangeable K indicates ongoing depletion of the element. Under such circumstances the probable process on the long term is release from the sparsely occurring K-bearing clay minerals, rather than fixation (Simonsson et al., 2007, 2009). Consequently, the negative end of the confidence interval for K-weathering can be dismissed. Also for Na, negative weathering is improbable considering the high solubility of this element in natural systems.

4.3. What should be done with the Type A and B uncertainties?

'Classical' Type A standard errors are often considered sufficient to use when testing whether treatment means in a replicated experiment are different. In order to make statements about absolute values, however, Type B uncertainties also need to be considered, e.g. in an effort to establish the largest off-take rates of base cations allowed in a sustainable forest management. Due to the marine influence at the Skogaby site, Mg and Na turned out to be sensitive to Type B uncertainties in deposition and leaching, whereas Ca and K appeared controlled by bioaccumulation, where Type B uncertainties were relatively unimportant. Although this classification of the ions is useful for the discussion below, it should not be inadequately generalised to sites in a different setting.

Table 7
Mean and combined standard uncertainty, $u_c(\text{Leach}_i)$, of the leaching of base cations . 'Type A only' is the standard error over the four plots, if Type B uncertainties were ignored; 'Type B' is the part of the combined standard uncertainty that derived from Type B uncertainties (cf. Table 2). Relative contributions (%) to $u_c\text{Leach}_i)$ were calculated in analogy with Eq. (6). Confidence intervals are shown in Fig. 1.

Statistics and contributions	Ca	Mg	K	Na	Cl	ΣBC
	($kg\ ha^{-1}\ yr^{-1}$) or %					($kmol_c\ ha^{-1}\ yr^{-1}$) or %
Mean	1.7	2.5	0.86	32	54	1.7
Combined standard uncertainty, $u_c(\text{Leach}_i)$	0.40	0.55	0.20	5.0	8.7	0.28
Type A only, SE(Leach_i)	0.36	0.49	0.18	3.9	6.7	0.22
Type B additional uncertainty, $u_{\text{Type B}}(\text{Leach}_i)$	0.17	0.25	0.09	3.2	5.4	0.17
Relative contributions to $u_c(Leach_i)$						
Type A: Between-plot $SE_{rel}(\text{Conc}_i)$	82%	80%	82%	59%	61%	63%
Type B: Estimated u_{rel}(Flux)	18%	20%	18%	41%	39%	37%

Table 8
Mean and combined standard uncertainty, $u_c(\text{Bioacc}_i)$, for the accumulation rate in biomass. 'Type A only' is the standard error over the four plots, if Type B uncertainties were ignored; 'Type B' is the part of the combined standard uncertainty that derived from Type B uncertainties (cf. Table 2). Relative contributions (%) to $u_c(\text{Bioacc}_i)$ were calculated in analogy with Eq. (6). Confidence intervals were calculated based on the combined standard uncertainty and a *t*-value of 3.18 (the 95-% level, 3 degrees of freedom).

Statistics and contributions	Ca	Mg	K	Σ(Ca, Mg, K)
	($kg\ ha^{-1}\ yr^{-1}$) or %			($kmol_c\ ha^{-1}\ yr^{-1}$) or %
Mean	7.4	2.8	4.2	0.71
Combined standard uncertainty, $u_c(\text{Bioacc}_i)$	1.7	0.33	1.4	0.13
Type A only	1.6	0.32	1.3	0.13
Type B, additional uncertainty, $u_{\text{Type B}}(\text{Bioacc}_i)$	0.5	0.10	0.3	0.04
Confidence interval (95%), Type A and B uncertainties	±5.4	±1.1	±4.3	±0.42
Relative contributions to $u_c(Bioacc_i)$				
Type A: Biomass, plot variability, $SE_{rel}(W_j)$	59%	76%	65%	76%
Type A: Concentration, partly generalised plot variability, $SE_{rel}(\text{Conc}_i)$	32%	14%	29%	14%
Type B: Biomass, allometric functions, $u_{rel,\ allometric}(W_j)$	3%	4%	4%	4%
Type B: Bark/stem ratio, u_{rel}(Bark/Stem)	5%	3%	2%	5%
Type B: Assumption stump-root conc, u_{rel}(Stump-root conc)	0.7%	2%	0.2%	0.9%

Our results indicate that "sufficiently high" standard errors may be obtained for cation accumulation in the biomass, even when ignoring Type B errors (Table 8). This is encouraging for similar ecosystem studies, because the calculations are considerably simplified if Type B uncertainties of allometric functions etc. can be ignored. The relative importance of Type A and B uncertainties depends on the circumstances of the studied experiment. With a greater number of plots, Type A standard errors would decrease, and with them the extended standard errors. As a consequence, the relative importance of several Type B uncertainties could be expected to increase, insofar as they do not depend on replication among plots.

To assess the often dominating flux of bioaccumulation, it is critical to use valid allometric functions. The use of generalised functions was justified in previous work on the Skogaby site, where it was found that the treatments did not differ significantly with respect to function parameters (Ågren, personal communication). Taking a wider perspective, possible bias in allometric functions for stumps and roots was not accounted for in the present study. The function that we used (Table 3) was developed by Petersson and Ståhl (2006) based on 31 specimens of *P. abies* from different parts of Sweden. In their comparison with previous results from Sweden, they found no systematic deviation of their function. Hence, it appeared possible to generalise the functions at least at a national scale.

If, in turn, bioaccumulation is a prominent term in the entire cation budget, this study's results for Ca and K suggest that a correct level of uncertainty may be obtained for estimated weathering rates, by using Type A uncertainties alone. Since both biomass and cation concentrations in tree tissues were critical for the combined uncertainty of bioaccumulation, it is important that plot-wise data for both variables are used.

If, on the other hand, deposition and leaching are prominent in the budget, our results for Mg and Na indicate that Type B uncertainties may be important. The discrepancy found between deposition and leaching of chloride also indicates that a correction for bias in either flux needs to be performed in each plot separately, to avoid systematic errors in the cation budget. The calculated weathering rate of Na was largely influenced by uncertainties in the leaching rate. The uncertainty of leaching, and the distribution of the error in leaching measurements, obviously needs further consideration in work on element budgets where leaching is a prominent term.

4.4. Predicting sustainability from cation budgets

In several field studies, the authors have assessed values for all fluxes, including weathering rates according to the PROFILE-model (Sverdrup and Warfvinge, 1993) or mineralogical considerations (Likens et al., 1998), and predicted the likely trends for exchangeable cations based on the balances obtained. In a recent compilation of data from the experimental Breuil-Chenue forest plantation established in 1976 in the Morvan, France, exchangeable Ca and K were relatively stable according to measurements in the soil, but should be depleted by 3 and 7 $kg\ ha^{-1}\ yr^{-1}$, respectively, according to cation budgets with weathering estimates obtained from PROFILE (van der Heijden et al., 2013). Whereas a discrepancy between observation and budget could be explained for Mg, the results for Ca and K suggest that the uncertainty in the cation budget was similar to the net balance itself. Laclau et al. (2005) assessed cation budgets and sustainability of a *Eucalyptus* plantation in Congo, where the modelled weathering input of base cations was negligible. Whereas depletion in soil nitrogen was highly probable, the data were not conclusive as to whether

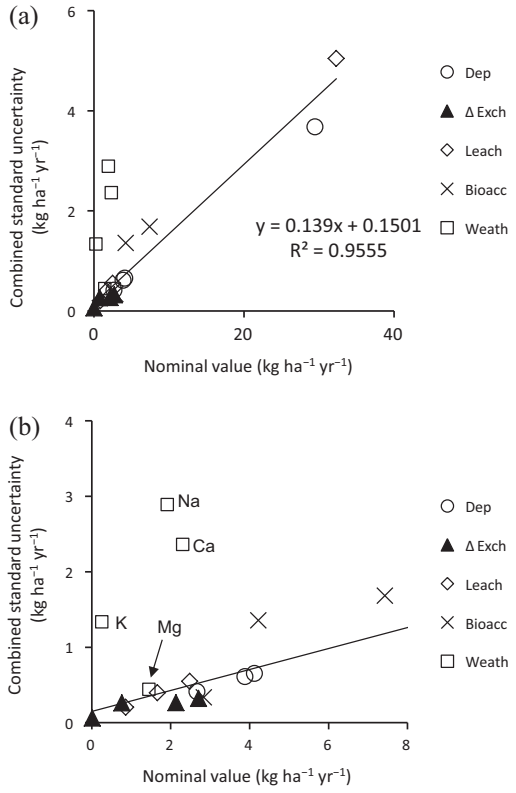

Fig. 6. Regression of combined standard uncertainties plotted against the modulus of average values for the cation budget terms (deposition input, change in exchangeable base cations, leaching and base cation accumulation in biomass; one point per cation for each term). In addition, weathering rates are shown for the four base cations, but not included in the regression. Figure (b) is a low-range close-up of (a). While the combined standard uncertainties of individual terms in the budget were roughly proportional to their nominal values, the weathering rates had considerably larger uncertainties compared to the nominal values.

exchangeable base cations were undergoing an increase or a decrease in the soil, primarily due to the uncertainties of deposition and accumulation in the harvested biomass, which were the most prominent fluxes.

In the national-scale study of Sverdrup et al. (2006), predicted changes in exchangeable K under conventional stem harvesting were mostly in the range of −2 to + 2 kg ha^{-1} yr^{-1}. Imbalances commonly corresponding to several kg ha^{-1} yr^{-1} were also found in the study of Sverdrup et al. (2006), which considered several tree species and a scale of several km^2. Fichter et al. (1998) calculated cation budgets for spruce and beech ecosystems at the hillslope scale and obtained negative balances, indicating a depletion of exchangeable base cations in the order of −0.4 to −3.7 kg ha^{-1} yr^{-1} for Ca, Mg, K and Na. In the Hubbard Brook Experimental Forest, the depletion of exchangeable Ca was calculated based on a mass balance for the watershed and mineralogical data (Likens et al., 1998). The calculated depletion during 1965–1992 was of the order 400–450 kg ha^{-1}, which was greater than the pool of exchangeable Ca in 1983 of 260 kg ha^{-1}. These pools and fluxes are almost tenfold greater than in the present paper.

Due to the way uncertainties of the terms accumulated in the cation budgets for Skogaby, weathering estimates for most elements suffered from a substantially greater uncertainty than the terms from which it was calculated (Fig. 6). It therefore appears that changes in exchangeable cations may be measured with higher precision, if assessed directly from soil data than via a cation budget. In the present data, confidence intervals for annual changes ranged from ±0.19 kg ha^{-1} yr^{-1} for Mg to ±1.0 kg ha^{-1} yr^{-1} for Ca. Although this represents a high precision compared to the studies cited above, it should be noted that the reported uncertainty is valid only for the current study period.

The analysis presented in this paper did not quantify the error when attempting to generalise the results for, e.g., an entire rotation period. Therefore, a discussion of the apparent abrupt changes in the pools of exchangeable cations seen in Fig. 3 is of some interest. If these changes were due to episodic fluxes to or from the soil, then the chosen time frame for the study period can be expected to have a large influence on the result. If, on the other hand, they were due to errors in sampling and laboratory procedures, then these uncertainties as such would need further consideration in similar studies. The data in Fig. 1 suggest that exchangeable Na had a mean residence time with respect to throughfall of only 1 year. The decline in exchangeable Na may be explained by an abrupt decrease in the deposition input, from 40–50 kg ha^{-1} yr^{-1} in 1989 and 1990, to 20–30 kg ha^{-1} yr^{-1} from 1991 and onwards (see Bergholm et al., 2003). The fluctuation patterns of exchangeable Ca, Mg and K, on the other hand, differed markedly from those of Na (Fig. 3). With a mean residence time of 3–4 years with respect to the gross uptake rates in Fig. 1, the exchangeable pools were likely to be influenced by fluxes between soil and vegetation. However, the low resolution in time and space of the present cation data for tree tissues does not allow us to study any variations in uptake rates over short periods. More detailed studies of cation budgets are needed to assess the credibility of variation patterns, such as those in Fig. 3.

Another concern is that changes in the pools of exchangeable cations might be a result not only of fluxes between soil and vegetation, but also of the dynamics of soil organic matter. Inputs of organic matter after a tree-felling have been reported to increase the stocks of exchangeable base cations in virtue of an increased abundancy of exchange sites in the soil profile (Johnson et al., 1997); the effect may persist for decades (Knoepp and Swank, 1997). During the thinning performed in 1993 at Skogaby, however, the above-ground biomass of felled trees was removed from the plots. Although there was a nearly significant decrease in the mass of the FH-layer over time (Section 3.2.2), the total stock of organic C in the forest floor and mineral soil remained at 100–110 ton ha^{-1} without significant changes during 1987–1997 according to measurements in the soil profile (Persson et al., 2001).

5. Conclusions

- Forest management on soils with a low ability to replenish harvested base cations through soil weathering is highly dependent on base cation cycling in the stand to support sustainable tree growth. This has implications for the suitability of intensified practices, such as whole tree harvesting and stump removal, on soils with a coarse texture and low weathering rates.
- Central values of weathering rates estimated from cation budgets at the Skogaby site were in the range of 0.3–2.4 kg ha^{-1} yr^{-1} for Ca, Mg and K in this study.
- Despite an ambitious sampling programme involving all relevant fluxes during the study period, the uncertainties, expressed as confidence intervals, were frequently greater than the central values themselves, and are likely to be so in similar studies on soils with low weathering rates due to limitations in texture or mineralogy.
- For cations where bioaccumulation dominates the budget (Ca and K in this study), a more or less correct level of uncertainty in weathering estimates is likely to be obtained merely by accounting for 'traditional' plot variability ('Type A' uncertainty), e.g. in biomass and cation concentrations in above-ground tree tissues. Uncertainties in functions and factors not

replicated over the plots ('Type B' uncertainties), such as allometric functions, appear to be of lesser importance, provided that the functions are representative of the studied forest stand.
- For cations with large deposition and leaching fluxes (Mg and Na in this study), it is necessary to take plot variability in throughfall (Type A uncertainty) into account, whereas this study's results indicate that the much smaller variability in open-field deposition is less critical. Regarding leaching estimates based on measured concentrations and modelled water fluxes, this study suggests that Type B uncertainties in the often used simulated water flux deserve further attention.

Acknowledgements

We are indebted to the many people engaged in establishing and running the Skogaby experiment over many years, and to two anonymous reviewers, who provided ideas and criticism that helped us develop the paper. Stephen Hillier at the James Hutton Institute in Aberdeen, Scotland, performed the analysis of quantitative bulk mineralogy. Rolf Danielsson in the Analytical Chemistry Group, Department of Chemistry at Uppsala University, provided advise and the spreadsheet solution to calculate combined standard uncertainties. The study was performed as part of the Environmental Monitoring and Assessment programme at SLU and the 'strong research environment' QWARTS (Quantifying Weathering rates for Sustainable Forestry), financed by the Swedish Research Council Formas (Grant No 2011-1691).

References

Akselsson, C., Westling, O., Sverdrup, H., Gundersen, P., 2007. Nutrient and carbon budgets in forest soils as decision support in sustainable forest management. Forest Ecol. Manage. 238, 167–174.
Andrist-Rangel, Y., Edwards, A.C., Hillier, S., Öborn, I., 2007. Long-term K dynamics in organic and conventional mixed cropping systems as related to management and soil properties. Agric. Ecosyst. Environ. 122, 413–426.
Bailey, S.W., Buso, D.C., Likens, G.E., 2003. Implications of sodium mass balance for interpreting the calcium cycle of a forested ecosystem. Ecology 84, 471–484.
Bain, D.C., Mellor, A., Robertson-Rintoul, M.S.E., Buckland, S.T., 1993. Variations in weathering processes and rates with time in a chronosequence of soils from Glen Feshie, Scotland. Geoderma 57, 275–293.
Baskerville, G.L., 1971. Use of logarithmic regression in the estimation of plant biomass. Can. J. For. Res. 2, 49–53.
Bélanger, N., Holmden, C., 2010. Influence of landscape on the apportionment of Ca nutrition in a Boreal Shield forest of Saskatchewan (Canada) using $^{87}Sr/^{86}Sr$ as a tracer. Can. J. Soil Sci. 90, 267–288.
Berg, B., Staaf, H., 1980. Decomposition rate and chemical changes of Scots pine needle litter. II. Influence of chemical composition. In: Persson, T. (Ed.), Coniferous Forests – An Ecosystem Study. Ecol. Bull., pp. 373–390.
Bergholm, J., Berggren, D., Alavi, G., 2003. Soil acidification induced by ammonium sulphate addition in a Norway spruce forest in southwest Sweden. Water Air Soil Pollut. 148, 87–109.
Bergholm, J., Jansson, P.-E., Johansson, U., Majdi, H., Nilsson, L.O., Persson, H., Rosengren-Brink, U., Wiklund, K., 1995. Air pollution, tree vitality and forest production – the Skogaby project. General description of a field experiment with Norway spruce in South Sweden. In: Nilsson, L.O., Hüttl, R.F., Johansson, U.T., Mathy, P. (Eds.), Nutrient Uptake and Cycling in Forest Ecosystems. Ecosystems Research Report 21. European Commission., pp. 69–87.
Calvaruso, C., Mareschal, L., Turpault, M.P., Leclerc, E., 2009. Rapid clay weathering in the rhizosphere of norway spruce and oak in an acid forest ecosystem. Soil Sci. Soc. Am. J. 73, 331–338.
Castrup, H., 2004. 8th Annual ITEA Instrumentation Workshop 5 May 2004, Lancaster, Ca. ITEA.
Courchesne, F., Gobran, G.R., 1997. Mineralogical variations of bulk and rhizosphere soils from a Norway spruce stand. Soil Sci. Soc. Am. J. 61, 1245–1249.
Eriksson, C.P., Holmgren, P., 1996. Estimating stone and boulder content in forest soils – evaluating the potential of surface penetration methods. Catena 28, 121–134.
FAO, 1990. FAO–UNESCO, Soil Map of the World. Revised Legend. Soils Bulletin 60. FAO, Rome.
Fichter, J., Dambrine, E., Turpault, M.P., Ranger, J., 1998. Base cation supply in spruce and beech ecosystems of the Strengbach catchment (Vosges Mountains, NE France). Water Air Soil Pollut. 104, 125–148.
Hillier, S., 1999. Use of an air brush to spray dry samples for X-ray powder diffraction. Clay Miner. 34, 127–136.
Hillier, S., 2003. Quantitative analysis of clay and other minerals in sandstones by X-ray powder diffraction (XRPD). Int. Assoc. Sedimentol. Spec. Publ. 34, 207–245.
Hodson, M.E., Langan, S.J., 1999. Considerations of uncertainty in setting critical loads of acidity of soils: the role of weathering rate determination. Environ. Pollut. 106, 73–81.
Holmqvist, J., Øgaard, A.F., Öborn, I., Edwards, A.C., Mattsson, L., Sverdrup, H., 2003. Application of the PROFILE model to estimate potassium release from mineral weathering in Northern European agricultural soils. Eur. J. Agron. 20, 149–163.
ISO, 1995. Guide to the Expression of Uncertainty in Measurement (GUM). ISO/IEC Guide 98:1995. International Organization for Standardization, Geneva, Switzerland.
Jansson, P.-E., 1998. Simulation Model and Heat Conditions. Description of the SOIL-Model. SLU, Uppsala, Sweden.
Johnson, C.E., Romanowicz, R.B., Siccama, T.G., 1997. Conservation of exchangeable cations after clear-cutting of a northern hardwood forest. Can. J. For. Res. 27, 859–868.
Klaminder, J., Lucas, R.W., Futter, M.N., Bishop, K.H., Köhler, S.J., Egnell, G., Laudon, H., 2011. Silicate mineral weathering rate estimates: are they precise enough to be useful when predicting the recovery of nutrient pools after harvesting? Forest Ecol. Manage. 261, 1–9.
Knoepp, J.D., Swank, W.T., 1997. Long-term effects of commercial sawlog harvest on soil cation concentrations. Forest Ecol. Manage. 93, 1–7.
Koseva, I.S., Watmough, S.A., Aherne, J., 2010. Estimating base cation weathering rates in Canadian forest soils using a simple texture-based model. Biogeochem. 101, 183–196.
Laclau, J.-P., Ranger, J., Deleporte, P., Nouvellon, Y., Saint-André, L., Marlet, S., Bouillet, J.-P., 2005. Nutrient cycling in a clonal stand of Eucalyptus and an adjacent savanna ecosystem in Congo 3. Input–output budgets and consequences for the sustainability of the plantations. Forest Ecol. Manage. 210, 375–391.
Likens, G.E., Driscoll, C.T., Buso, D.C., Siccama, T.G., Johnson, C.E., Lovett, G.M., Fahey, T.J., Reiners, W.A., Ryan, D.F., Martin, C.W., Bailey, S.W., 1998. The biogeochemistry of calcium at Hubbard Brook. Biogeochem. 41, 89–173.
Lövblad, G., Persson, C., Roos, E., 2000. Deposition of base cations in Sweden. Swedish Environmental Protection Agency, Report No 5119. Naturvårdsverket, Stockholm.
Mead, R., Curnow, R.N., Hasted, A.M., 1993. Statistical Methods in Agriculture and Experimental Biology. Chapman & Hall, London.
Nilsson, L.-O., Östergren, M., Wiklund, K., 2001. Hur påverkades träden ovan mark? In: Persson, T. and Nilsson, L.-O. (Eds.), Skogabyförsöket: Effekter av långvarig kväve- och svaveltillförsel till ett skogsekosystem. Swedish Environmental Protection Agency, Report 5173, Stockholm, pp. 51–66.
Nilsson, L.O., Wiklund, K., 1994. Nitrogen uptake in a norway spruce stand following ammonium-sulfate application, fertigation, irrigation, drought and nitrogen-free-fertilization. Plant Soil 164, 221–229.
Öborn, I., Edwards, A.C., Hillier, S., 2010. Quantifying uptake rate of potassium from soil in a long-term grass rotation experiment. Plant Soil 335, 3–19.
Olsson, B.A., Bengtsson, J., Lundkvist, H., 1996. Effects of different forest harvest intensities on the pools of exchangeable cations in coniferous foret soils. Forest Ecol. Manage. 84, 135–147.
Olsson, M., Melkerud, P.A., 1989. Chemical and mineralogical changes during genesis of a Podzol from till in Southern Sweden. Geoderma 45, 267–287.
Olsson, M.T., Melkerud, P.-A., 2000. Weathering in three podzolized pedons on glacial deposits in northern Sweden and central Finland. Geoderma 94, 149–161.
Omotoso, O., Mccarty, D.K., Hillier, S., Kleeberg, R., 2006. Some successful approaches to quantitative mineral analysis as revealed by the 3rd Reynolds Cup contest. Clays Clay Miner. 54, 748–760.
Perakis, S.S., Maguire, D.A., Bullen, T.D., Cromack, K., Waring, R.H., Boyle, J.R., 2006. Coupled nitrogen and calcium cycles in forests of the Oregon coast range. Ecosyst. 9, 63–74.
Persson, T., Bergholm, J., Nilsson, L.-O., Majdi, H., 2001. Kolförrådet ovan och under mark i Skogaby. In: Persson, T. and Nilsson, L.-O. (Eds.), Skogabyförsöket: Effekter av långvarig kväve- och svaveltillförsel till ett skogsekosystem. Swedish Environmental Protection Agency, Report 5173, Stockholm, pp. 78–84.
Petersson, H., Ståhl, G., 2006. Functions for below-ground biomass of *Pinus sylvestris*, *Picea abies*, *Betula pendula* and *Betula pubescens* in Sweden. Scand. J. For. Res. 21, 84–93.
Rothpfeffer, C., Karltun, E., 2007. Inorganic elements in tree compartments of *Picea abies*—concentrations versus stem diameter in wood and bark and concentrations in needles and branches. Biomass Bioenergy 31, 717–725.
Simonsson, M., Andersson, S., Andrist-Rangel, Y., Hiller, S., Mattsson, L., Öborn, I., 2007. Potassium release and fixation as a function of fertilizer application rate and soil parent material. Geoderma 140, 188–198.
Simonsson, M., Hillier, S., Öborn, I., 2009. Changes in clay minerals and potassium fixation capacity as a result of release and fixation of potassium in long-term field experiments. Geoderma 151, 109–120.
Sposito, G., 1989. The Chemistry of Soils. Oxford University Press, New York.
Stendahl, J., Akselsson, C., Melkerud, P.-A., Belyazid, S., 2013. Pedon-scale silicate weathering: comparison of the PROFILE model and the depletion method at 16 forest sites in Sweden. Geoderma 211–212, 65–74.
Stendahl, J., Lundin, L., Nilsson, T., 2009. The stone and boulder content of Swedish forest soils. Catena 77, 285–291.
Sverdrup, H., Thelin, G., Robles, M., Stjernquist, I., Sörensen, J., 2006. Assessing nutrient sustainability of forest production for different tree species considering Ca, Mg, K, N and P at Björnstorp Estate, Sweden. Biogeochem. 81, 219–238.

Sverdrup, H., Warfvinge, P., 1993. Calculating field weathering rates using a mechanistic geochemical model PROFILE. Appl. Geochem. 8, 273–283.
Thiffault, E., Hannam, K.D., Paré, D., Titus, B.D., Hazlett, P.W., Maynard, D.G., Brais, S., 2011. Effects of forest biomass harvesting on soil productivity in boreal and temperate forests – a review. Environ. Rev. 19, 278–309.
Turpault, M.P., Righi, D., Uterano, C., 2008. Clay minerals: Precise markers of the spatial and temporal variability of the biogeochemical soil environment. Geoderma 147, 108–115.
van der Heijden, G., Legout, A., Pollier, B., Mareschal, L., Turpault, M.-P., Ranger, J., Dambrine, E., 2013. Assessing Mg and Ca depletion from broadleaf forest soils and potential causes – a case study in the Morvan Mountains. Forest Ecol. Manage. 293, 65–78.
Viro, P.J., 1952. On the determination of stoniness. Comm. Inst. Forest. Fenn. 40, 1–23.
Yanai, R.D., Battles, J.J., Richardson, A.D., Blodgett, C.A., Wood, D.M., Rastetter, E.B., 2010. Estimating uncertainty in ecosystem budget calculations. Ecosyst. 13, 239–248.